

## Observed tidal currents on the continental shelf off the west coast of India

M.P Subeesh<sup>\*1</sup>, A.S. Unnikrishnan<sup>1</sup>, V. Fernando<sup>1</sup>, Y. Agarwadekar<sup>1</sup>, S.T. Khalap<sup>1</sup>, N.P.Satelkar<sup>1</sup> and S.S.C. Shenoi<sup>2</sup>

1. CSIR-National Institute of Oceanography, Dona Paula, Goa, India, 403004

2. Indian National Centre for Ocean Information Services (INCOIS), Ocean Valley, Pragathi Nagar (BO), Nizampet (SO), Hyderabad, 500090

\* Corresponding Author

Email: [subeeshoceanography@gmail.com](mailto:subeeshoceanography@gmail.com); Phone: +91-832-2450400 (office)

### Abstract

Observed currents from ADCPs, deployed at 100 meter and 150 meter depths, on the continental shelf at five different locations along the west coast of India, were used to study the characteristics of both barotropic and baroclinic tidal currents. The observations extended over a six-month period (March to August), which includes two seasons, pre-monsoon (March-April) and southwest monsoon (SW) (May-August) during 2008, 2009 and 2011. Tidal ellipses, constructed for  $M_2$  and  $K_1$  constituents, show that barotropic tidal currents propagate in along-isobath direction at southern shelf (off Kollam at about  $9^{\circ}$  N) and they are oriented more or less in cross-isobath direction at northern shelf locations (off Jaigarh and Mumbai at about  $17^{\circ}$  N and  $20^{\circ}$  N respectively). Maximum cross-isobath tidal current is found at northern shelf locations (for instance, about  $32 \text{ cm s}^{-1}$  off Mumbai) than those in south (about  $10 \text{ cm s}^{-1}$  off Bhatkal, at  $13^{\circ}$  N). This could be due to the amplification of semidiurnal tidal constituents from south to north of the shelf due to an increase in shelf widths towards north. The rotary spectra of baroclinic currents showed large peaks at semidiurnal and diurnal bands with a dominant clockwise rotation showing the presence of strong internal currents. Semidiurnal variability occurs mainly in  $M_2$  and  $S_2$  and diurnal variability occurs mainly in  $K_1$  and  $O_1$ . An increase in the amplitude of semidiurnal and diurnal internal tide is apparent when the stratification on the shelf increases from pre-monsoon to SW monsoon period. The presence of strong internal tide during May to August is attributed to increased seasonal stratification on the shelf. EOF analysis showed that the first three modes are sufficient to describe most of the variability in both semidiurnal and diurnal internal tide on the shelf, as they represent about 70-90% of total variance. The small scale vertical shear in the velocity field, induced by diurnal internal tide, is found to be larger than that induced by semidiurnal internal tide.

**Key words:** barotropic tidal currents; baroclinic tidal currents; ADCP; continental shelf; eastern Arabian Sea

## 1. Introduction

Both barotropic and baroclinic tidal currents have been widely studied around the world ocean particularly on the continental shelves and slopes (for example, Huthnance, 1989; Holloway et al., 2001; Xu et al., 2011b, 2013). The astronomical forcing mainly leads to the generation of barotropic tidal currents, while baroclinic tidal currents, commonly called internal tides, are caused by the interaction of barotropic tidal flow with topography in the presence of stratification and they propagate in onshore as well as offshore directions. Internal tides have temporal scales from inertial to local Brunt-Väisälä frequency ( $f < \sigma < N$ ), where  $\sigma$  is the internal wave frequency and  $f$  and  $N$  are inertial and buoyancy frequencies respectively. The direct astronomical forcing in the generation of internal tides is negligible. The variability of internal tide can be largely modified by background stratification (Aguirre et al., 2010; Bravo et al., 2013; Green et al., 2010; Rosenfield, 1990). On a continental shelf internal tidal currents play an important role in the dynamics, by producing vertical shear (Xu et al., 2011b), mixing across the shelf (Rippeth and Inall., 2002), re-suspension of bottom sediments (Bogucki et al., 1997; Butman et al., 2006), controlling continental margin ecosystems (Sharples et al., 2009) etc.

The continental shelf off the west coast of India is very narrow on the southern side, with a gradual northward widening (Figure 1). For example, starting from south, the shelf widens from about 85 km off Kochi (about  $9^{\circ}$  N) to about 230 km off Mumbai coast (about  $20^{\circ}$  N). North of the Gulf of Khambhat, the shelf width reduces to about 110 km (about  $21^{\circ}$  N). The co-tidal charts prepared using global tidal models indicate that the tides in the Arabian Sea propagate from south to north (Lyard et al., 2006). The amplitudes of major tidal constituents along the west coast (Table 1) show that tidal range is low in the south and it increases towards north. The tides are found to be mixed semidiurnal type in the southern part of the shelf (see the last column of Table 1), and become more semidiurnal type further north (eg., at Mumbai). Large tidal range (about 3 m during spring tide), with semi-diurnal dominance, was reported on the mid-shelf off Mumbai, based on the measurements of water surface elevations made from a drilling platform for oil and natural gas (Joseph et al., 2009).

The seasonal variability of hydrography and circulation on the continental shelf off the eastern Arabian Sea were described in earlier studies (Shetye et al., 1990; Shetye et al., 1991a). However, a description of tidal currents in the Arabian Sea has received little attention so far. One study that deals with observed tidal currents in the mid Arabian Sea (near  $14^{\circ}$  N and  $64^{\circ}$  E) is that of Shenoi et al., (1992), who analyzed nearly one year-long current meter observations. They estimated the velocity of

$M_2$  barotropic tidal current as  $1.2 \text{ cm s}^{-1}$  to  $1.6 \text{ cm s}^{-1}$ , which are similar in magnitude to those observed in mid-Atlantic and mid-Pacific (Magaard and McKee, 1973; Weisberg et al., 1987).  $K_1$  tidal current in the location is found to have magnitudes of  $0.89 \text{ cm s}^{-1}$ .

On the shelf of the eastern Arabian Sea, only a few studies have described the tidal currents. The main reason is the absence of sufficiently long measurements of currents on the shelf. Though short records are available at some locations over the region, they are insufficient to describe the spatial variability of tidal currents. However, the short-duration records provided high-frequency wind-driven currents (Varkey, 1980; Unnikrishnan and Antony, 1990; Shenoi and Antony, 1991; Antony and Shenoi, 1993; Shetye et al., 2008) and limited information on major tidal constituents (Shenoi et al., 1988, 1994; Fernandes et al., 1993). Shenoi et al., (1988) found strong semidiurnal barotropic and baroclinic signal off Goa ( $15^\circ \text{ N}$ ) by using 8-day current meter observations. Later, Shenoi et al., (1994) studied the variation of barotropic and baroclinic  $M_2$  constituent off Goa in detail, using short term (about 10 days) RCM observations, which was available for different months (March, May and November). The study addressed seasonal variation of  $M_2$  internal tide and found that  $M_2$  baroclinic current is dominated by the first mode and their values are equal to or higher than barotropic tidal currents. Fernandes et al., (1993) described the tidal currents on the mid-shelf in Mumbai High region using a ten-day current meter record during winter and found that currents at different depths are identical. Later, Unnikrishnan et al., (1999) simulated the aforementioned currents using a vertically integrated hydrodynamic model, driven by tides and showed that the circulation in the region is driven primarily by barotropic tides. The large variability of temperature fields caused by predominant internal tides has also been reported in earlier works (Murthy and Hareesh Kumar, 1991; Unnikrishnan and Antony, 1990; Hareesh Kumar et al., 2006; Hareesh Kumar et al., 2010).

Arabian Sea experiences mainly two seasons, the South West (SW) monsoon (May-September) and the North East (NE) monsoon (November-January). The ADCP data covered months of March to August, that is, the period of pre-monsoon (March-April) and most of the SW monsoon months (May-August). Hydrography on the shelf shows distinct patterns during NE and SW monsoons, which are associated with downwelling and upwelling. On the shelf, no significant signal of coastal upwelling has been reported during March. Weak upwelling is developed in early April off Kochi ( $9^\circ \text{ N}$ ) and off Mangalore (about  $12^\circ \text{ N}$ ) (Shenoi et al., 2005) and it gets strengthened during May onwards and becomes well developed during June to September. An equatorward upwelling gradient is present in the

north eastern Arabian Sea (Shetye et al., 1990). This occurs because upwelling forms in the south at first and the signal progressively propagates to the north of the shelf (Shankar and Shetye, 1997). Upwelling causes shallowing of the mixed layer and increases the vertical gradient of density of water column. The highly stratified layer may enhance the internal wave activity on the shelf (Hareesh Kumar et al., 2010). However, strong upwelling may cause vertical mixing of the water column and may decay the internal waves (Aruirre et al., 2010; Rosenfield, 1990).

In this paper, we present the description of tidal currents on the shelf off the west coast of India based on the data obtained through long term measurements of currents using self recording ADCPs, moored at five locations along the shelf (Figure 1). Amol et al., (2012) and Vialard et al., (2009) used these records or part of those to describe the intra-seasonal variability of coastal currents in the region. The high quality observations from these ADCP moorings provide a unique opportunity to look into the tidal variability, which has not been done so far. The shelf off the west coast of India exhibits strong seasonal variations in the stratification and consequently the internal tidal currents are also expected to vary with seasons. This study presents a description of characteristic features associated with both barotropic and baroclinic tidal currents along the shelf off the west coast of India, for the two seasons, the pre-monsoon (March-April) and the SW monsoon (May-August).

The present paper is organized as follows. In section 2, we describe the data and methods used in this study. Section 3 presents the results followed by discussion and conclusions in section 4.

## **2. Data and methods**

The data were collected using upward looking RDI Acoustic Doppler Current Profilers (ADCP, 300 kHz) which were deployed on the shelf, near the 100 m isobaths, off the west coast of India (Figure 1). In addition to those in the shelf, the ADCPs were also moored on the slope. However, the data from the shelf were only used for the present analysis. There were 5 moorings (Table 2) on the shelf, which are separated by a distance of about 150 to 200 km. There were two ADCP deployments off Kollam ( $9^{\circ}$  N), one was at about 100 m depth and the other at 150 m depth. The first data set was not included in the present analysis because more than 40% of water column near the surface had missing values. We chose ADCP at 150 m off Kollam, since it had good values of about 80% of the water column after removing all contaminated data. Missing values off Bhatkal and Goa are 18% and 19%, respectively, while those at Jaigarh and Mumbai are 34% and 40% respectively. Off Mumbai, about 25% of values in bottom water column became blank due to ADCP positioning. All other ADCPs were placed just above the

bottom using a short taut mooring so that the ADCP looks upward over the entire water column. The sampling was done at each 4 m level in vertical and the temporal sampling interval was 15 minutes, except off Kollam, where sampling interval was 30 minutes with the same 4 m vertical interval. The accuracy of velocity measurements was better than  $1.55 \text{ cm s}^{-1}$  (Amol et al., 2012). Table 2 provides the duration of the available data. Data were not available close to the surface owing to contamination of data due to echoes. All data were available mostly downward of 15 m from the surface. The velocity data from ADCP records, after careful quality checks, were used to analyse the tidal currents along the shelf.

A six-month period of observation (March-August) was picked from different years (2008, 2009 and 2011) for the analysis as it provides an opportunity to look at the seasonal variation of tidal currents. The period includes two seasons, pre-monsoon (March-April) and SW monsoon (May-August). We divided the raw data into three subsections of two months each, March-April, May-June and July-August, based on the density structure on the shelf. Vertical density structure obtained from climatology does not show considerable difference between these two-month periods (Details of density structure are given in the next section). Various analyses were carried out for three subsections. The barotropic currents were obtained through vertically averaging the raw velocity field. By excluding the top and bottom boundary layers, depth averaging the measured velocity provides a good estimate of barotropic velocity. The bottom boundary layer is anyway excluded, as the ADCP is positioned at least 10 m above the bottom and the data from  $\sim 8$  m above the position of ADCP are non-usable due to blanking. The surface data (about 10 to 15 m) was also removed due to contamination. The abrupt fluctuations in the velocities of raw currents were examined carefully and removed. The rest of the velocity field were averaged vertically for each subsection separately and considered as barotropic currents. Subsequently, the baroclinic currents were obtained by subtracting the barotropic currents from raw current. The time series of both barotropic and baroclinic currents (U and V components) thus obtained were then subjected to harmonic analysis using TASK (Tidal analysis and Software Kit) software package (Bell et al., 1998) to extract the tidal constituents. The ellipse parameters for different constituents of both barotropic and baroclinic tides were estimated and tidal ellipses were constructed.

The current vectors were rotated with respect to the orientation of isobaths for all analysis carried out subsequently (Table 2 gives the angle of rotation at each location). Hence, the terms ‘along-isobath’ and ‘cross-isobath’ currents indicate the rotated tidal currents. Rotary spectra of baroclinic currents were

calculated to obtain clockwise and anticlockwise components. The baroclinic currents were band passed between 0.8 cpd and 4 cpd, using a third-order Butterworth filter, to retain baroclinic tidal currents and also band passed them for semidiurnal (1.8-2.2 cpd) and diurnal (0.8-1.2 cpd) internal tide. Empirical Orthogonal Function (EOF) analysis was carried out for semidiurnal and diurnal internal tides separately to determine the vertical modes. Vertical shear is calculated for above bands to further characterize internal tides.

### **3. Results**

#### **3.1. Current spectra**

To describe the characteristics of high frequency currents on the shelf, we computed variance spectra of cross-isobath and along-isobath raw currents at near surface, mid-depth and bottom over the entire six month period (Figures 2 and 3). The current spectra show prominent peaks at near-inertial frequency and tidal frequencies. Off Kollam, at the southernmost shelf location, tidal energy is predominant in the along-isobath direction (Figure 3). Tidal energy tends to be more oriented in the cross-isobath direction further north (off Bhatkal). At Bhatkal, both peaks in cross-isobath and along-isobath at tidal frequencies have nearly the same energy. Further north, cross-isobath tidal energy is stronger than that of along-isobath. The maximum difference between the cross-isobath and along-isobath energy is found on the shelf off Jaigarh (Figures 2 and 3). In tidal spectra, significant peaks are found at frequencies of  $M_2$ ,  $S_2$  and  $N_2$  (semidiurnal) and  $K_1$  and  $O_1$  (diurnal). The energy of each constituent varies along the shelf. Generally,  $M_2$  is found to be the most prominent peak in all locations. Off Bhatkal,  $M_2$  has less energy at near surface and at bottom it gets reversed, where significant bottom amplification of  $M_2$  is apparent. Though  $O_1$  is weak compared to other constituents, off Mumbai, it has a significant peak (Figure 2). No substantial difference in diurnal energy peaks is found from surface to mid-depth and bottom, except off Goa, where diurnal energy is weaker at bottom. Compared to other locations, semidiurnal energy is stronger in the northern shelf locations (off Jaigarh and Mumbai). Near inertial wave energy is also significant on the shelf, which is present in a broad frequency band. In the present paper, our focus is mainly on the variability in the tidal frequency bands.

#### **3.2. Stratification on the shelf**

The vertical section of sigma-t across each mooring point on the shelf is shown (Figure 4). Density was calculated from the revised climatology of temperature and salinity atlas of the North

Indian Ocean (Chatterjee et al., 2011). During SW monsoon, high discharge from various rivers and excess precipitation cause increased stratification on the shelf region. Moreover, coastal upwelling occurring off the west coast of India during the SW monsoon (Shetye and Shenoi, 1988; Shetye et al., 1990) also determines the density structure of water column. Upwelling is discernible from May onwards off the southwest coast of India, and extends northward along the coast with the progress of monsoon (Rao et al., 2008). Upwelling signal off Goa ( $15^{\circ}$  N) has been reported in July but as a weak signal and it was observed to be intense during September (Antony and Unnikrishnan, 1992). During March and April, the isopycnals are quasi-horizontal or slightly bending down towards the coast, which shows weak stratification over the shelf during this period (Figure 4). From May onwards, the water column becomes stratified. During June, at the southern location (off Kollam), isopycnals are found to be bending upwards. The upward tilt of isopycnals is visible off Goa and Bhatkal from July onwards only. During August and September, upwelling is found to be maximum in the above three locations. No significant upwelling signal is noticeable on the shelf off Jaigarh and Mumbai during the period of deployment (Figure 4). With the progress of upwelling towards north, stratification of water column gradually increases.

### **3.3. Barotropic tidal currents**

The amplitudes of major tidal constituents obtained through the harmonic analysis applied to the full records of cross-isobath and along-isobath barotropic currents are shown in Table 3. In the hierarchy of tidal constituents driving the barotropic tidal currents over the shelf off the west coast of India, the  $M_2$  constituent is the largest, followed by  $K_1$ ,  $S_2$ ,  $N_2$  and  $O_1$ .  $K_1$  and  $S_2$  have nearly comparable amplitudes while  $O_1$  is the weakest among them (off Kollam  $N_2$  is the weakest constituent). Off Jaigarh,  $S_2$  is the second largest constituent. The amplitudes of semidiurnal constituents are found to be larger off Jaigarh and Mumbai compared to those in the southern locations (Table 3). The comparison of amplitudes of cross-isobath and along-isobath components of major tidal constituents shows that the cross-isobath component of barotropic tides tend to increase towards north. Off Kollam, near the southern tip of the shelf, the tidal currents are oriented clearly in along-isobath direction. But, off Bhatkal, both components have more or less same magnitudes. Further north, off Goa, Jaigarh and Mumbai, the cross-shore component is stronger than that of along-isobath component.

The relationship between eastward (U) and northward (V) components of barotropic currents is described in terms of ellipses. We determined the ellipses of  $M_2$  and  $S_2$  for semidiurnal (Figure 5a) and

$K_1$  and  $O_1$  for diurnal constituents (Figure 5b). Ellipses were constructed for different two-month periods of data to check the temporal stability of barotropic tidal currents. Ellipse parameters of the above constituents for each time-period are shown in Table 4. As seen from Figure 5, amplitudes of semidiurnal constituents do not vary appreciably with time, except off Kollam, where  $M_2$  ellipse gets slight amplification in July-August period (Table 4). Off Mumbai and Bhatkal  $K_1$ , ellipses vary from March-April to those in May-August. We also computed barotropic tidal constituents using entire velocity records (not shown). We compared the values of semi-major axis obtained from successive two-month data segments and the values obtained from the entire observation period. Most of  $M_2$  and  $S_2$  amplitudes obtained from former analysis vary within 10 % from those obtained from the latter analysis. In March-April, ellipses of diurnal constituents off Mumbai and Bhatkal show 20-40% of variation of amplitude between the two analyses. Semi-major axes of  $K_1$  and  $S_2$  ellipses are about 40-60% those of  $M_2$ . It is found that  $S_2/M_2$  ratio is 0.4 to 0.6 on the shelf, which shows a pronounced spring-neap cycle. Velocity vector consistently rotates in clockwise direction, as expected in the Northern Hemisphere. At the southernmost location, off Kollam, the major axis of the ellipses of all the major constituents is oriented quasi-parallel to the isobaths. Off Bhatkal, the orientation of ellipses differs for different constituents. For example, the  $K_1$  ellipse is inclined north-south (quasi-parallel to isobaths) while those of  $M_2$  and  $S_2$  are oriented east-west (quasi-perpendicular to isobaths). Further north, off Jaigarh and Mumbai, where shelf widths are larger than in the south, the ellipses are oriented more or less perpendicular to the isobaths. The semidiurnal tidal ellipses in these locations are much larger than those in the south.

### **3.4. Internal Tidal Currents**

#### **3.4.1. Internal tides time series**

Figure 6 shows the time evolution of cross-isobath internal tidal currents during a 15 day observation in March and July. Variance profile for March and July is also shown (Figure 6c). Baroclinic currents, band passed between 6 to 30 hrs are considered as internal tidal currents. This frequency band excludes inertial energy (The inertial period is 76.7 hrs and 35.0 hrs at  $9^{\circ}$  N and at  $20^{\circ}$  N respectively), which is present substantially along the shelf. Internal tides on the shelf are intermittent in nature with irregular temporal variability. Figure 6a and b show considerable difference between the amplitudes of internal tide from March to July. From the right panel of Figure 6, it is clear that internal tide variance exhibits seasonal variability. Internal tides are found to be weak during March, when the



stratification is weak over the shelf. During July, when the stratification is high, internal tides are found to be strong. Current-reversal always occurred at mid-depths (40-60 m, except off Kollam, where it occurred at 70-100 m depth) suggesting that current velocity is dominated by the first baroclinic mode motion in all the locations. Off Kollam, especially in March, the vertical structure is more complex, where higher mode motions may also be significant. We performed EOF analysis for a detailed description of the vertical structure of baroclinic tidal currents on the shelf, which is described in section 3.4.6.

### 3.4.2. Rotary spectra

Figure 7 shows the result of rotary spectra of baroclinic currents at about 20 m depth during March to April and July to August. Clockwise (CW) spectrum dominated anticlockwise (ACW) spectrum in all internal tide and near-inertial frequencies, consistent with propagation in Northern Hemisphere. This shows the presence of strong internal and near-inertial current on the shelf. Large and broad peaks appear in the spectra of inertial currents with significant difference between CW and ACW energy (polarity, which is the ratio of CW and ACW, is greater than one). Though near-inertial currents are significant on the shelf, we restricted our discussion to tidal currents in the present paper. In the tidal band, an energetic peak occurs at  $M_2$  frequency with apparent clockwise rotation. Other than  $M_2$ , prominent peaks observed in semidiurnal are  $S_2$  and  $N_2$ . Spectra show prominent peaks at diurnal frequencies,  $K_1$  and  $O_1$ . Off Jaigarh and Kollam, diurnal band contributes to significant energy. Off Kollam, the difference between CW and ACW spectra is small in  $K_1$  (polarity is less than one). Off Goa and Bhatkal, CW component of diurnal internal tide energy is weaker compared to those in other locations. Other peaks emerge at higher harmonics like,  $M_4$  and  $M_2+O_1$  but comparatively with less energy.  $M_2+O_1$  peaks are caused by the combination of semidiurnal and diurnal tides because of nonlinear interaction and advection of major diurnal and semidiurnal tides (Xu et al., 2013). Figure 7a & b indicate seasonal variation of  $M_2$ . Generally, during pre-monsoon period, CW component of  $M_2$  energy is found to be weak and its energy strengthens in SW monsoon period (Figure 7). During pre-monsoon, its energy is found to be weaker than those in near inertial (at all locations) and diurnal (Off Mumbai, Jaigarh and Kollam) frequencies. However, off Goa,  $M_2$  energy is found to be stronger during pre-monsoon and there is no substantial strengthening of energy between spectra of March to April and July to August (Figure 7). There is no considerable strengthening of energy in the diurnal spectra from pre-monsoon to the SW monsoon.

### 3.4.3. $M_2$ ellipses

To investigate the vertical structure of semidiurnal internal tide and its seasonal variation we constructed  $M_2$  baroclinic ellipses for all available depths at different seasons. Figure 8 shows the ellipses of  $M_2$  internal tide obtained through harmonic analysis on baroclinic velocity for each two month period (March-April, May-June, and July-August). As seen from the previous section (Figure 7), semidiurnal and diurnal internal tide spectra are broad, which include  $M_2$ ,  $N_2$ , and  $S_2$  (semidiurnal) and  $K_1$  and  $O_1$  (diurnal) frequencies. In semidiurnal frequencies,  $M_2$  is the largest constituent in all locations, followed by  $S_2$  and  $N_2$ . For example, during SW monsoon,  $S_2$  contributes 40-60% of  $M_2$  internal tide to the total for all the locations (except off Kollam, where  $S_2$  is found to be very small). In this section, we used  $M_2$  ellipses to describe semidiurnal variability on the shelf.

Maximum value of semi-major axis of  $M_2$  is found on the shelf off Mumbai (about  $8 \text{ cm s}^{-1}$ ). Velocity maxima are always found in either near surface or near bottom depths (Figure 8). Seasonal variation of  $M_2$  internal tide is apparent on the shelf. For example, semi-major axis of  $M_2$  off Mumbai varies from  $1 \text{ cm s}^{-1}$  to  $8 \text{ cm s}^{-1}$  during pre-monsoon to SW monsoon (Figure 8a). It is interesting that, during most of the period of observation,  $M_2$  internal tide is strong on the shelf off Goa. Even in pre-monsoon season,  $M_2$  internal tide was found to be strong (Maximum value of semi-major axis is about  $5 \text{ cm s}^{-1}$ ) on the shelf off Goa. Here,  $M_2$  internal tide strengthened during May to June and it weakened in July to August (Figure 8c). To find out the month at which  $M_2$  internal tide is really weakening, we conducted a running one-month harmonic analysis (not shown) of baroclinic currents off Goa. This analysis shows that the  $M_2$  internal tides are strong in July and weak in August. Maximum value of semi-major axis off Goa during August is  $2 \text{ cm s}^{-1}$  which is much smaller than those during July, when the corresponding value is  $6 \text{ cm s}^{-1}$ .

Most of the  $M_2$  baroclinic ellipses are aligned in cross-isobath direction. The baroclinic  $M_2$  ellipses off Mumbai and Jaigarh (Figure 8a & b) are aligned in the same direction of its barotropic ellipses (Figure 5). The internal tidal ellipses are oriented in the same direction of energetic barotropic ellipses here. Off Goa,  $M_2$  ellipses are oriented more in cross-isobath than its barotropic counterpart (Figure 8c). Off Bhatkal also,  $M_2$  ellipses are well aligned across the isobaths, where ellipses are slightly inclined to the south of the barotropic ellipses. In both locations, during the time of strong internal tide,  $M_2$  internal tide exceeded the barotropic  $M_2$  currents. For instance, at near surface, semi-major axis of  $M_2$  internal tide off Goa (Bhatkal) during May to June is  $5.73 \text{ cm s}^{-1}$  ( $5.71 \text{ cm s}^{-1}$ ) which is higher than

those of barotropic ellipses which are  $5.3 \text{ cm s}^{-1}$  ( $4.52 \text{ cm s}^{-1}$ ). This is more or less visible in other semidiurnal constituents such as  $S_2$  and  $N_2$ , and not visible in diurnal constituents. For example, off Goa, at near surface, semidiurnal  $S_2$  (about  $3 \text{ cm s}^{-1}$ ) and  $N_2$  (about  $4 \text{ cm s}^{-1}$ ) show larger amplitude than its barotropic counterpart ( $1.5 \text{ cm s}^{-1}$  and  $1.8 \text{ cm s}^{-1}$ ).

The length of semi-major axis is always found to be minimum at about 50 m depth (Figure 8), except, off Kollam, where those are found to be around 70 m (Figure 8e). That is, the minimum amplitudes of ellipses are always found at mid-depth of water column. Figure 8b, c & d show that, depth of minimum amplitude of  $M_2$  ellipses varies slightly between two-month periods, probably with the seasonal variation of pycnocline. Most of the  $M_2$  ellipses rotate in clockwise direction, as expected for the internal tidal currents in the Northern Hemisphere. However, off Kollam, tidal ellipses tend rotate anticlockwise in different depths (Figure 8e).

#### **3.4.4. $K_1$ ellipses**

In diurnal internal tidal constituents, the largest is  $K_1$  followed by  $O_1$ .  $K_1$  ellipses are weakest off Goa and Bhatkal and strongest off Kollam. Off Kollam,  $K_1$  has comparable magnitude to  $M_2$  (Maximum velocity of  $K_1$  is found about  $6 \text{ cm s}^{-1}$ , for  $M_2$  it is about  $5.9 \text{ cm s}^{-1}$ ) (Figure 9e). Here ellipses are oriented mostly in along-isobath direction. The sense of rotation is predominantly anticlockwise here during the time of SW monsoon. Off Mumbai and Jaigarh, during pre-monsoon, internal tides are found to be stronger in  $K_1$  than in  $M_2$  (Figure 8 & 9). Diurnal constituents also show variation in vertical structure of ellipses in different seasons, though not as prominent as in semidiurnal. We will describe the details of seasonal variation of diurnal internal current in following section. The absence of velocity minima at mid-depths suggests that the vertical structure of  $K_1$  (Figure 9) is more complex than that of  $M_2$  (Figure 8).  $O_1$  is not shown since it is found to be small and the semi-major axis never exceeded  $3.0 \text{ cm s}^{-1}$  at any depths and for any other location except off Kollam.

#### **3.4.5. Temporal variation**

To further address temporal variation of internal tide, we calculated depth-averaged variance ( $u^2+v^2$ ) for both semidiurnal (1.8-2.2 cpd) and diurnal bands (0.8-1.2 cpd) separately, which is shown in Figure 10. We also calculated two-month averaged (March-April and July-August) semidiurnal and diurnal baroclinic current variance ( $\langle u^2 \rangle + \langle v^2 \rangle$ ) with depth (Figure 11). Prior to the analysis, a third order butter worth filter was used to extract the semidiurnal and diurnal bands from rotated baroclinic

currents. Semidiurnal and diurnal internal tides exhibit spring-neap modulations (Figure 10) and seasonal variations. Semidiurnal internal tides are stronger in SW monsoon than those during pre-monsoon, which is consistent with the previous analysis. The shelf exhibits monthly and seasonal variations in diurnal internal tide also. Off Goa and Bhatkal, diurnal kinetic energy is weak during the observation period. The strengthening of internal tide is not consistent during all the months of SW monsoon. The semidiurnal and diurnal variance tends to weaken from mid-July to August off Goa and from June to mid-July off Bhatkal. Minimum variance of internal tide is always found at mid-depths (Figure 11). Off Mumbai, during March-April, internal tides are stronger in diurnal band than in semidiurnal. Diurnal wind is well developed along the Indian west coast during February-April (Aparna et al., 2005). However, there is no near surface amplification of diurnal internal tide during these months (March-April) (Figure 11), when land-sea breeze are present, indicating that the role of diurnal wind on the generation of internal tide may not be significant.

#### **3.4.6. EOF analysis**

EOF analysis was used to decompose the baroclinic tidal currents into vertical modes of variance. Prior to this, the cross-isobath component ( $U'$ ) and along-isobath component ( $V'$ ) of baroclinic currents for different two-month periods were band passed for semidiurnal (1.8-2.2 cpd) and diurnal (0.8-1.2 cpd) internal tide. The time series obtained were then decomposed into various vertical modes (Figure 12 & 13). To explain the seasonal variability of vertical structure of internal tides, we show the results of EOF analysis for representative pre-monsoon (March-April) and SW monsoon (July-August) periods separately.

The analysis showed that the first three modes are sufficient to describe most of the variability in both semidiurnal and diurnal internal tide on the shelf, as they represent about 70-90% of total variance. The contribution from higher modes is much small and not shown. On the shelf both semidiurnal and diurnal internal tides are dominated by the first mode (Figure 12 & 13). Mostly the vertical pattern of first mode velocity of  $V'$  is similar to those of  $U'$  but with weaker amplitudes. The variance of each mode varies from pre-monsoon to SW monsoon and also between observations points. Variances of first mode semidiurnal internal tide increase from pre-monsoon to SW monsoon in all locations. On the northern shelf, off Mumbai, the first mode accounts for nearly 80% of cross-isobath semidiurnal internal tide during SW monsoon, this is only about 69% during pre-monsoon. Off Kollam, variance of first mode semidiurnal (diurnal) is only about 58% (48%) during SW monsoon and second mode explains

15% (23%) of the total variance (Figure 12). This shows that the vertical pattern of internal tide is more complex on the shelf off Kollam. Variance of second mode cross-isobath diurnal internal tides is slightly higher than that of semidiurnal. This indicates that diurnal internal tide has more complex vertical structures than that of semidiurnal. The zero-crossing of the first mode lies between 40 and 60 m. However, off Kollam, first mode zero-crossing lies between 70 and 100 m. Off Jaigarh, zero-crossing point of first mode diurnal internal tide changes from 40 m to 60 m from pre-monsoon to SW monsoon, which is more or less consistent with vertical pattern of  $K_1$  ellipses (Figure 8). The modal structure of the first mode obtained from EOF analysis more or less agrees with the vertical pattern of ellipses from previous harmonic analysis for all locations.

#### **3.4.6. Shear analysis**

Figure 13 shows the vertical shear  $((\delta u/\delta z)^2 + (\delta v/\delta z)^2)$  field caused by the semidiurnal and diurnal band of internal currents. The baroclinic tides induced small-scale vertical shear in the velocity fields on the shelf. The intermittent vertical shear is noticed at all locations in semidiurnal and diurnal bands. Shear induced by semidiurnal baroclinic tidal current is comparatively weaker than that due to diurnal. Semidiurnal shear is found to be large at mid-depths of the water column (40-60 m), where the current reversal occurs. Diurnal shear spreads at different levels of water column. As seen in the previous section (Figures 12 & 13), semidiurnal and diurnal internal tide is dominated by the first mode, where the zero crossing is found at mid-depths. This is consistent with shear maxima, which are also found at mid-depths. However, vertical structure of diurnal internal tide is more complex (Figures 12 & 13), where higher mode motions are also substantial, and these induce shear at different levels of water column.

### **4. Discussion and Conclusion**

Observations from five ADCP moorings along the shelf off the west coast of India revealed the presence of significant barotropic tidal currents on the shelf associated with varying internal tidal current in different frequencies. Current spectra show narrow band signal at four tidal frequencies ( $M_2$ ,  $S_2$ ,  $K_1$  and  $O_1$ ), and a broad frequency band at near inertial frequencies.

#### **Barotropic tidal current**

In the southernmost location (Kollam), tidal currents propagate clearly in along-isobath direction. This could be due to the entry of tide into the Arabian Sea from south and its propagation

towards north. Further north, tidal currents tend to be oriented in a cross-isobath direction. On the northern part of the shelf (off Mumbai and Jaigarh) barotropic tidal currents are strong. Semidiurnal tidal currents are found to be stronger on the northern part of the shelf (off Mumbai and Jaigarh) and they contribute most of the energy to the barotropic current. It is found that, from off Goa to Jaigarh, semi-major axis of semidiurnal barotropic tidal ellipses are amplified about three times. This shows that the semidiurnal barotropic tidal currents considerably increase towards the north, specifically from narrow shelves to wider shelves (Figure 5a). But, diurnal tidal currents do not show significant variation from south to north (Figure 5b). Shelf width plays an important role in the amplification of semidiurnal tidal current off Mumbai and Jaigarh. In fact, the present study is insufficient to describe the causes of the amplification of semidiurnal barotropic tide from south to north. We intend to carry out a numerical modelling which will help to explain the spatial variations in tidal currents.

### **Internal tidal current**

The detailed analysis of the tidal currents off west coast of India, using long term mooring revealed the presence of strong internal tides on the shelf, which are confined mostly to semidiurnal and diurnal periods. The baroclinic tidal currents on the shelf show variations in amplitude and in its vertical structure from pre-monsoon to monsoon periods. Formation or generation of internal tide requires density stratification as a prerequisite. From May onwards stratification on the shelf increases, where isopycnals are quasi parallel and the surface density is low. A strong thermocline, sandwiched between upper and bottom homogenous layer (Tri-layer structure) is common in Indian coastal waters off the west coast during SW monsoon (Hareesh Kumar et al., 2005, 2006). This may enhance the internal tide generation on the shelf. Hareesh Kumar (2010) showed that the degree of vertical stratification and the amplitude of high frequency internal tide are directly related on the shelf of northeast coast of India ( $22.13^{\circ}$  N and  $68.62^{\circ}$  E). This may be true for all the locations discussed in this study, where internal tide amplitudes are directly related to the seasonal density variation on the shelf. In general, the amplitude of internal tides shows a tendency to increase with increasing stratification, as noted elsewhere on the shelf region of the world ocean (for instance, Holloway, 1984; Huthnance and Baines, 1982).

Though the amplification of  $M_2$  internal tide from March-April to May-June is observed in Goa, there is a dampening of  $M_2$  observed during July-August. Off Goa, upwelling becomes stronger from August onwards (Antony and Unnikrishnan, 1992), which may tend to cause the water column to be

homogenous and inhibit the generation of internal tide to some extent. This feature has been noted in other regions, especially in upwelling sites (Aguirre et al., 2010; Rosenfeld, 1990). This feature is not verified as we do not have real time temperature and salinity data during the time of ADCP observations.

During the period of strong internal tide off Goa, Bhatkal and Kollam, cross-isobath  $M_2$  internal tides are found to be larger in magnitude than their barotropic counterparts. But at the same time, for the along-isobath component, the barotropic component is prominent. This is found in other semidiurnal constituents and not in diurnal constituents. This lack of coherence in the cross-isobath and along-isobath component could be due to the difference in the generation mechanisms of internal tidal currents. The cross-isobath component of semidiurnal internal tidal current might be generated due to the incidence of barotropic tide at the slope region and then directed towards the shore. On the other hand, the along-isobath component of internal current might be generated due to the direct forcing locally. These results are complementary to the results of Shenoi et al., (1988), who described the mechanism of generation of semidiurnal internal tide off Goa. Off Jaigarh and Mumbai, barotropic tidal currents are found to be more energetic than internal tide.

The first mode baroclinic current is dominated by  $M_2$  which contributes significant energy to internal tide. Our study shows that baroclinic tidal currents in most of the locations are dominated by the cross-shelf propagating first mode  $M_2$  as reported on many other shelf regions (Holloway, 1983, 1984; Sherwin, 1988). However, off Kollam, internal tidal currents are weaker in cross-isobath direction compared to along-isobath direction. Relatively weak cross-isobath barotropic forcing component could be one reason for the weak cross-isobath internal tide here. Higher mode internal tidal currents are also significant in different locations. The exact generation site of these internal currents is unknown and rather difficult to explain using the available data. Higher modes of internal tidal current present in semidiurnal and diurnal internal tides are probably generated on the shelf or from nearby regions, since small vertical scale waves cannot propagate far from the source of generation (St. Laurent and Garrett, 2002).

We performed different analyses to examine the contribution of diurnal wind to the observed, and baroclinic tidal currents. If the response of diurnal wind is found up to mixed layer (Rosenfeld, 1988), or penetrate below the mixed layer (Lerczak et al., 2001 ) we expect surface- enhanced diurnal current. If the forcing is from the surface, and not from tide, it is also expected that lines of constant phase will

propagate towards the surface (downward energy flux) (Lerczak et al., 2001). We found that there is no upward phase propagation and surface-enhanced diurnal current on the shelf. So we concluded that the contribution of diurnal wind on diurnal current is not significant in the location of moorings and during the period of observation. However, ADCP data were not available for depths less than 15 m. If the response of diurnal wind is confined to upper layer of less than 15 m, it is rather impossible to resolve its contribution in surface layers using the available data set. We need measurements of winds and currents in the upper layers of the water column to estimate response of the diurnal wind on the currents in the surface layers.

During the occurrence of strong internal tidal currents, shear is evolving at different depth levels intermittently (Figure 14). Small scale vertical shear is present at different depth levels due to semidiurnal and diurnal internal tidal currents, with a maximum found at mid-depth. In surrounding depth levels shear is possibly generated by the superposition of different vertical modes of internal tide. In fact, the barotropic and baroclinic currents over the shelf off the west coast of India are complex in nature. We intend to carry out numerical modelling studies to explain the observed characteristics of tidal currents in this region.

## **5. Acknowledgements**

The funding for ADCP deployment was provided by Council of Scientific and Industrial Research (CSIR) and Indian National Center for Ocean Information Services (INCOIS) (Ministry of Earth Sciences). The first author thanks UGC for his research fellowship. We thank Dr S. R. Shetye and Dr D. Shankar for providing valuable suggestions. All figures in this paper were made using Generic Mapping Tools and the analysis was done using Ferret and MATLAB. We also thank the officers, crew, and seamen on the mooring cruises for providing the necessary support for deploying the ADCPs. We are grateful to USGS for providing their ADCP toolbox (<http://woodshole.er.usgs.gov/operations/stg/pubs/ADCPtools/adcpindex.htm>). The USGS MATLAB code was converted to Octave and C by A. Krishnakiran, R. Fernandes, S.P. Vernekar, and N. Nasnodkar. The manuscript also benefited from comments and suggestions by two anonymous reviewers. This is NIO Contribution No XXXX.



## References

- Aguirre, C., Pizarro, O., Sobarzo, M., 2010. Observations of semi diurnal internal tidal currents off central Chile [36.6° S]. *Continental Shelf Research* 30, 1562–1574.
- Amol, P., Shankar, D., Aparna, S.G., Shenoi, S.S.C., Fernando, V., Shetye, S.R., Mukherjee, A., Agarvadekar, Y., Khalap, S., Satelkar, N.P., 2012. Observational evidence from direct current measurement for propagation of remotely forced waves on the shelf off the west coast of India. *Journal of Geophysical Research* 117, 15.
- Antony, M.K., Shenoi, S.S.C., 1993. On the flow, thermal field and winds along the western continental shelf of India. *Continental Shelf Research* 13, 425–439.
- Antony, M.K., Unnikrishnan, A.S., 1992. On an upwelling front, propagation of upwelling and vertical velocity in the eastern Arabian sea during monsoon, 1987. *Proceedings of the PORSEC '92 in Okinawa, Conference for Pacific Ocean Environments and Probing* 1, 527-532.
- Aparna, M., Shetye, S.R., Shankar, D., Shenoi, S.S.C., Mehra, P., Desai, R.G.P 2005. Estimating the seaward extent of sea breeze from QuikSCAT scatterometry. *Geophysical Research Letters* 32, L13601, doi:10.1029/2005GL02310.
- Bell, C., Vassie, J., Woodworth, P., 1998. POL/PSMSL Tidal Analysis Software Kit 2000 (TASK-2000). Tech. rep., Proudman Oceanography Lab., Bidston Observatory, Merseyside, U.K.
- Bogucki, D., Dickey, T., Redekopp, L.G., 1997. Sediment resuspension and mixing by resonantly generated internal solitary waves. *Journal of Physical Oceanography* 27, 1181-1196.
- Bravo, L., Ramos, M., Sobarzo, M., Pizarro, O., Valle-Levinson, A., 2013. Barotropic and baroclinic semidiurnal tidal currents in two contrasting coastal upwelling zones of Chile. *Journal of Geophysical Research* 118, 1–13, doi:10.1002/jgrc.20128.
- Butman, B., Alexander, P.S., Scotti, A., Beardsley, R.C., Anderson, S.P., 2006. Large internal waves in Massachusetts Bay transport sediments offshore. *Continental Shelf Research* 26, 2029 – 2049.
- Chatterjee, A., Shankar, D., Shenoi, S.S.C., Reddy, G.V., Michael, G.S., Ravichandran, M., Gopalkrishna, V.V., Rao, E.P.R., Bhaskar, T.V.S.U., Sanjeevan, V.N., 2012. New atlas of temperature and salinity for North Indian Ocean. *Journal of Earth System Science* 121(3), 559–593.
- Fernandes, A.A., Chandramohan, P., Nayak, B.U., 1993. Observed currents at Bombay High during a winter. *Mahasagar* 26(2), 95-104.
- Green, J.A.M., Simpson, J.H., Thorpe, S.A., Rippeth, T.P., 2010. Observations of internal tidal waves in the isolated seasonally stratified region of the western Irish Sea. *Continental Shelf Research* 30, 214–225.
- Hareesh Kumar, P.V., Pradeep Kumar, T., Sunil, T., Gopakumar., M., 2005. Observations on the relationship between scattering layer and mixed layer. *Current Science* 88, 1799–1802.

- Hareesh Kumar, P.V., Sanilkumar, K.V., Panchalai, V.N., 2006. Shallow water internal waves and associated acoustic intensity fluctuations. *Defence Science Journal* 56, 485–493.
- Hareesh Kumar, P.V., Lekshmi, S., Jagadeesh, P.S.V., Anilkumar, K., Krishnakumar, G.V., Rao, A.D., 2010. Internal Tides in the Coastal Waters of NE Arabian Sea: Observations and Simulations. *Marine Geodesy* 33:2-3, 232-244.
- Holloway, P.E., 1983. Internal tides on the Australian North West Shelf: A preliminary investigation. *Journal of Physical Oceanography* 13, 1357-1370.
- Holloway, P. E., 1984. On the semidiurnal internal tide at a shelf-break region on the Australian North West Shelf. *Journal of Physical Oceanography* 14, 1787-1799.
- Holloway, P., Chatwin, P., Craig, P., 2001. Internal tides observations from the Australian North West shelf in summer 1995. *Journal of Physical Oceanography* 31, 1182–1199.
- Huthnance, J.M., Baines, P.G., 1982. Tidal currents in the northwest African upwelling region. *Deep Sea Research* 29, 285-306.
- Huthnance, J.M., 1989. Internal tides and waves near the continental shelf edge. *Geophysical and Astrophysical Fluid Dynamics* 48, 81-106.
- Joseph, A., Vijay Kumar, K., Mehra, P., Unnikrishnan, A.S., Sundar, D., Desai, R.G.P., 2009. Observed tides at Mumbai High offshore region, near the continental shelf break in the eastern Arabian Sea. *Current Science* 96(9), 1233-1235.
- Lerczak, J.A., Hendershott, M.C., Winant, C.D., 2001. Observations and modeling of coastal internal waves driven by a diurnal sea breeze. *Journal of Geophysical Research* 106, 0148-0227.
- Lyard, F., Lefevre, F., Letellier, T., Francis, O., 2006. Modelling the global ocean tides: modern insights from FES2004. *Ocean Dynamics* 56, 394–415.
- Magaard, L., McKee, W.D., 1973. Semidiurnal tidal currents at ‘site D’. *Deep-Sea Research* 20, 997-1009.
- Murthy, P.G.K., Hareesh Kumar, P.V., 1991. Respects of coastal waters off Karwar to a deep depression. *Continental Shelf Research* 3, 239–250.
- Rao, A.D., Joshi, Madhu., Ravichandran, M., 2008. Oceanic upwelling and downwelling processes in waters off the west coast of India. *Ocean Dynamics*. doi:10.1007/s10236-0080147-4.
- Rippeth, T.P., Inall, M.E., 2002. Observation of internal tide and associated mixing across the Malin shelf. *Journal of Geophysical Research* 107, C4, 3028.
- Rosenfeld, L.K., 1988. Diurnal period wind stress and current fluctuations over the continental shelf off northern California. *Journal of Geophysical Research* 93, 2257–2276.

- Rosenfeld, L.K., 1990. Baroclinic semidiurnal tidal currents over the continental shelf off northern California. *Journal of Geophysical Research* 95, 22153–22172.
- Sharples, J., Moore, C.M., Hickman, A.E., Holligan, P.M., Tweddle, J.F., Palmer, M.R., Simpson, J.H., 2009. Internal tidal mixing as a control on continental margin ecosystems. *Geophysical Research Letters* 36, L23603, doi:10.1029/2009GL040683.
- Shankar, D., Shetye, S.R., 1997. On the dynamics of the Lakshadweep high and low in the southeastern Arabian Sea. *Journal of Geophysical Research (C: Oceans)* 102, 12,551–12,562.
- Shenoi, S.S.C., Antony, M.K., Sundar, D., 1988. Nature of the observed oscillatory flows in shelf waters of the western continental shelf of India. *Journal of Coastal Research* 4, 617–626.
- Shenoi, S.S.C., Antony, M.K., 1991. Current measurements over the western continental shelf of India. *Continental Shelf Research* 11, 81–93.
- Shenoi, S.S.C., Gouveia, A.D., Shetye, S.R., 1992. Diurnal and Semidiurnal tidal currents in the deep mid-Arabian sea. *Proceedings of the Indian Academy of Science (Earth and planetary sciences)* 101, 177–189.
- Shenoi, S.S.C., Gouveia, A.D., Shetye, S.R., 1994.  $M_2$  tidal currents on the shelf off Goa, west coast of India. *Ocean Technology perspectives*, 415–427.
- Shenoi, S.S.C., Shankar, D., Michael, G.S., Kurian, J., Varma, K.K., RameshKumar, M.R., Almeida, A.M., Unnikrishnan, A.S., Fernandes, W.A., Barreto, N., Gnanaseelan, C., Mathew, R., Praju, K.V., Mahale, V.P., 2005b. Hydrography and water masses in the southeastern Arabian Sea during March–June 2003. *Journal of Earth System Science* 114, 475–491.
- Sherwin, T., 1988. Analysis of an internal tide observed on the Malin shelf, North of Ireland. *Journal of Physical Oceanography* 18, 1035–1050.
- Shetye, S.R., Gouveia, A.D., Shenoi, S.C.C., Sundar, D., Michael, G.S., Almeida, A.M., Santanam, K., 1990. Hydrography and circulation off the west coast of India during the southwest monsoon 1987. *Journal of Marine Research* 48, 359–378.
- Shetye, S.R., Gouveia, A.D., Shenoi, S.S.C., Michael, G.S., Sundar, D., Almeida, A.M., Santanam, K., 1991. The coastal current off western India during the northeast monsoon. *Deep-Sea Research* 38, 1517–1529.
- Shetye, S.R., Shenoi, S.C.C., 1988. Seasonal cycle of surface circulation in the coastal north Indian Ocean. *Proceedings of the Indian Academy of Science (Earth and Planetary Sciences)* 97, 53–62.
- Shetye, S.R., Suresh, I., Shankar, D., Sundar, D., Jayakumar, S., Mehra, P., Desai, R.G.P., Pednekar, P.S., 2008. Observational evidence for remote forcing of the west India coastal current. *Journal of Geophysical Research (C: Oceans)* 113, C11001, doi:10.1029/2008JC004874.
- Sindhu, B., Suresh, I., Unnikrishnan, A.S., Bhatkar, N.V., Neetu, S., Michael, G.S., 2007. Improved bathymetric data sets for the shallow water regions in the Indian Ocean. *Journal of Earth System*

Science 116, 261–274.

- St. Laurent, L., Garrett, C., 2002. The role of internal tides in mixing the deep ocean. *Journal of Physical Oceanography* 32, 2882-2899.
- Unnikrishnan, A.S., Antony, M., 1990. On vertical velocity fluctuations and internal tides in an upwelling region off the west coast of India. *Estuarine, Coastal and Shelf Science* 31, 865–873.
- Unnikrishnan, A.S., Shetye, S.R., Michael, G.S., 1999. Tidal propagation in the Gulf of Khambhat, Bombay High, and surrounding areas. *Proceedings of Indian Academy of Science (Earth and Planetary Sciences)* 108 (3), 155-177.
- Varkey, M.J., 1980. Power spectra of currents off Bombay. *Indian Journal of Marine Sciences* 9, 278–280.
- Vialard, J., Shenoi, S.S.C., McCreary, J.P., Shankar, D., Durand, F., Fernando, V., Shetye, S. R., 2009. Intraseasonal response of the Northern Indian Ocean coastal waveguide to the Madden-Julian oscillation. *Geophysical Research Letters* 36, L14606, doi:10.1029/2009GL038450.
- Weisberg, R.H., Halpern, D., Tang, T.Y., Hwang, S.M., 1987.  $M_2$  tidal currents in the eastern equatorial Pacific Ocean. *Journal of Geophysical Research* 92, 3821–3826.
- Xu, Z., Yin, H.B.S., Hou, Y.J., 2011b. Multimodal structure of the internal tides on the continental shelf of the northwestern South China Sea. *Estuarine, Coastal and Shelf Science* 95, 178-185, doi:10.1016/j.ecss.2011.08.026.
- Xu, Z., Yin, H.B.S., Hou, Y.J., Xu, Y., 2013. Variability of internal tides and near-inertial waves on the continental slope of the northwestern South China Sea. *Journal of Geophysical Research* 118, 197–211.

**Table 1:** Amplitude (A) and Phase (g) of five major tidal constituents ( $M_2$ ,  $S_2$ ,  $N_2$ ,  $K_1$  and  $O_1$ ). The phase is with respect to Greenwich. The final column given the ‘form number ( $F = \frac{K_1 + O_1}{M_2 + S_2}$ )’ of the tide at each station.

Location	Latitude ( <sup>0</sup> N)	Longitude ( <sup>0</sup> E)	$M_2$		$S_2$		$N_2$		$K_1$		$O_1$		$F_{-}$
			A (cm)	g ( <sup>0</sup> )	A (cm)	G ( <sup>0</sup> )	A (cm)	g (cm)	A (cm)	g ( <sup>0</sup> )	A (cm)	g ( <sup>0</sup> )	
Mumbai	18.92	69.97	123.0	345.0	048.0	025.0	029.0	326.0	042.0	055.0	020.0	052.0	0.36
Ratnagiri	16.98	73.30	066.3	317.2	026.3	355.8	015.0	297.0	034.5	053.6	016.1	057.2	0.55
Marmagao	15.41	73.80	056.0	312.0	020.0	350.0	013.0	292.0	031.0	054.0	016.0	051.0	0.62
Bhatkal	13.96	74.53	035.7	325.0	026.2	016.0	006.1	309.0	024.4	058.0	007.6	049.0	0.52
Cochin	09.97	76.26	020.0	346.0	007.0	047.0	004.0	319.1	017.0	064.0	009.0	065.0	0.96

**Table 2:** Locations of the moorings and the period of deployment.

ADCP No	Mooring Location	Position		ADCP Depth (m)	Water Depth (m)	Coastal angle ( <sup>0</sup> )	Start date	End date
		Latitude ( <sup>0</sup> N)	Longitude ( <sup>0</sup> E)					
M100	Mumbai	20.91	69.23	79	112	20.91	21/Oct/08	12/Sep/09
J100	Jaigarh	17.15	72.08	92	108	36.00	04/Mar/08	18/Oct/08
G100	Goa	15.17	73.19	90	98	21.40	02/Mar/08	22/Oct/08
B100	Bhatkal	13.67	73.51	97	104	16.94	05/Mar/08	07/Sep/08
K150	Kollam	09.00	75.96	154	179	30.57	20/Sep/10	25/Oct/11

**Table 3:** The amplitude of different barotropic tidal constituents, obtained from the harmonic analysis for the entire period of records of cross-isobath and along-isobath barotropic currents. All constituents larger than  $1 \text{ cm s}^{-1}$  are shown in the table.

Constituents	Mumbai		Jaigarh		Goa		Bhatkal		Kollam	
	U ( $\text{cm s}^{-1}$ )	V ( $\text{cm s}^{-1}$ )	U ( $\text{cm s}^{-1}$ )	V ( $\text{cm s}^{-1}$ )	U ( $\text{cm s}^{-1}$ )	V ( $\text{cm s}^{-1}$ )	U ( $\text{cm s}^{-1}$ )	V ( $\text{cm s}^{-1}$ )	U ( $\text{cm s}^{-1}$ )	V ( $\text{cm s}^{-1}$ )
$M_2$	13.34	5.71	17.58	2.85	5.01	2.36	4.11	3.44	2.26	8.73
$S_2$	5.58	2.55	7.15	1.40	1.81	1.33	1.79	1.61	1.23	3.63
$N_2$	3.77	1.69	4.37	0.77	1.21	0.48	0.85	0.62	0.56	1.76
$K_1$	6.02	3.81	4.84	1.83	1.91	1.08	2.43	3.00	2.39	5.22
$O_1$	2.4	1.68	3.28	1.20	0.96	0.49	1.03	0.93	1.21	3.07

**Table 4:** Barotropic ellipse parameters for major tidal constituents  $M_2$ ,  $S_2$ ,  $K_1$  and  $O_1$ .

	March-April				May-June				July-August			
	semi-major ( $\text{cms}^{-1}$ )	Semi-minor ( $\text{cms}^{-1}$ )	Angle (deg)	Phase (deg)	Semi-major ( $\text{cms}^{-1}$ )	Semi-minor ( $\text{cms}^{-1}$ )	Angle (deg)	Phase (deg)	semi-major ( $\text{cms}^{-1}$ )	Semi-minor ( $\text{cms}^{-1}$ )	Angle (deg)	Phase (deg)
<b>Mumbai</b>												
$M_2$	13.80	04.96	17.2	303.1	13.34	05.52	013.0	302.7	13.20	05.70	009.1	311.2
$S_2$	05.24	02.09	015.0	338.6	06.36	02.43	001.8	337.5	05.68	02.74	009.7	336.8
$K_1$	08.11	05.58	016.3	357.8	05.29	03.30	023.8	004.2	05.15	02.90	014.6	353.6
$O_1$	02.92	02.16	043.7	343.6	01.91	01.14	027.8	340.1	02.49	01.51	011.5	356.3
<b>Jaigarh</b>												
$M_2$	18.15	02.26	041.7	240.8	17.70	02.68	039.9	241.4	17.01	02.57	039.8	240.8
$S_2$	07.00	01.30	040.0	240.8	06.90	01.80	041.2	281.1	07.34	00.89	040.3	271.1
$K_1$	04.96	01.06	041.1	301.1	05.03	02.49	045.1	304.6	04.55	01.40	042.4	292.7
$O_1$	02.09	01.00	049.4	295.9	02.46	01.23	36.94	278.4	02.91	01.54	040.1	296.7
<b>Goa</b>												
$M_2$	05.12	01.85	219.7	038.7	05.36	02.10	031.2	223.0	05.06	01.85	220.9	039.1
$S_2$	01.90	00.48	038.4	259.4	01.83	01.20	036.3	252.4	02.05	01.43	244.7	046.6
$K_1$	01.48	00.79	036.4	323.3	02.72	01.39	032.6	322.5	02.45	00.84	074.6	320.5
$O_1$	01.38	00.74	056.6	326.1	00.83	00.08	038.5	312.3	01.12	00.35	018.7	310.4
<b>Bhatkal</b>												
$M_2$	04.97	01.23	232.7	032.1	04.52	00.82	229.6	029.3	06.05	01.92	244.5	022.5
$S_2$	02.01	00.59	070.8	259.5	03.24	01.85	044.0	238.3	02.08	00.97	238.9	044.6
$K_1$	01.32	00.69	065.2	336.0	04.44	02.61	061.6	316.2	05.05	02.61	082.5	336.1
$O_1$	02.33	00.80	106.9	004.7	01.72	00.52	038.2	303.3	02.15	01.20	040.9	308.4
<b>Kollam</b>												
$M_2$	08.88	01.20	301.1	09.33	08.03	0.75	282.5	08.23	09.87	03.80	293.7	014.7
$S_2$	03.17	00.56	292.5	037.3	04.17	2.03	275.7	047.9	04.32	01.48	305.2	046.2
$K_1$	05.08	00.94	089.1	304.9	06.34	1.31	099.5	307.6	05.33	01.25	102.1	304.2
$O_1$	02.66	00.09	092.5	296.6	03.81	0.80	105.4	285.6	03.60	00.02	101.2	303.9

**Figure 1:** ADCP mooring location off the west coast of India. M100, J100, G100, B100, K150 are different moorings on the shelf at 100 m and 150 m water depth. The depth contours are shown (Sindhu et al., 2007), where black (grey) contour shows 100 m (150 m) isobath. The inset map is the entire Indian Ocean.

**Figure 2:** Variance-preserving spectra of tidal and inertial currents from cross-isobath observed currents at near surface (about 20 m), middle, and bottom depths. 20 m was chosen as near-surface data, which is the depth at which data were available at all locations. Vertical lines indicate the different frequencies. Theoretical inertial frequency ( $f=2\omega\sin(\Phi)$ , where  $\omega$  is the angular frequency of rotation of the earth and  $\Phi$  is the latitude) is also shown in figure.

**Figure 3:** Same as above but for along-isobath currents.

**Figure 4:** The vertical structure of sigma-t across the ADCP mooring locations for March to August. The density data were calculated from the revised climatology data of North Indian Ocean (Chatterjee et al., 2011). Triangle indicates the location of moorings on the shelf. Contour interval is 0.5.

**Figure 5:** The spatial distribution of (a) semidiurnal (black (dotted) circle is  $M_2$  ( $S_2$ )); (b) diurnal (black (dotted) circle is  $K_1$  ( $O_1$ )) barotropic tidal ellipses along the shelf. Ellipses are obtained from the two month subsection analysis as indicated in figure label. Locations A (Mumbai), B (Jaigarh), C (Goa), D (Bhatkal) and E (Kollam) are shown. The sense of rotation of all ellipses is clockwise. The 100 m and 50 m depth contours are also shown.

**Figure 6:** Band-pass filtered (6-30 hrs) cross-isobath internal tidal currents during (a) March and (b) July. The observation period chosen for the analysis comprise the first spring and neap cycle of barotropic tidal current of the respective month. Variance of internal tide in March and July ( $\langle u^2 \rangle + \langle v^2 \rangle$ ), where bracket indicates one-month average) is also shown on the right panel.

**Figure 7:** Clockwise and anticlockwise spectra of baroclinic currents at near surface (about 20 m) for all locations. Red color represents clockwise part and black color represents anticlockwise part. Left panel is for the pre-monsoon months (March-April). Right panel is SW monsoon months (July- August). Theoretical inertial frequency ( $f=2\omega\sin(\Phi)$ ) is also shown in figure.

**Figure 8:** Baroclinic  $M_2$  current ellipses at different depths from running two month harmonic analysis for the different moorings. MA indicates March-April, which is representative pre-monsoon month, MJ,



JA indicate May-June and July-August which are the representative SW monsoon months. All ellipses, except those grey colored, rotate clockwise. Grey color indicates anticlockwise rotation.

**Figure 9:** Same as Figure 8 but for  $K_1$ .

**Figure 10:** Time series of baroclinic current variances ( $u^2+v^2$ ) at semidiurnal (1.8-2.2 cpd) and diurnal (0.8-1.2 cpd) frequency bands.

**Figure 11:** Average semidiurnal (1.8-2.2 cpd) and diurnal (0.8-1.2 cpd) bands variance ( $\langle u^2 \rangle + \langle v^2 \rangle$ ) versus depth for pre-monsoon (March-April) and SW monsoon (July-August). Dotted (Thick) line indicates the variance for March-April (July-August).

**Figure 12:** EOF analysis of cross-isobath semidiurnal and diurnal baroclinic tidal currents for different locations for two month periods: (a) pre-monsoon (March-April) (b) SW monsoon (July-August) is shown. The vertical structure of first three modes for semidiurnal internal tide is shown in left panels and same for diurnal internal tide is shown in right panels.

**Figure 13:** Same as Figure 12 but for along-isobath baroclinic tidal currents.

**Figure 14:** Time evolution of the vertical shear ( $s^{-1}$ ) of semidiurnal and diurnal baroclinic tidal currents. We chose the first 15 day period starting from July 1<sup>st</sup> to estimate the variations in shear field. Shear is calculated over 4m interval.

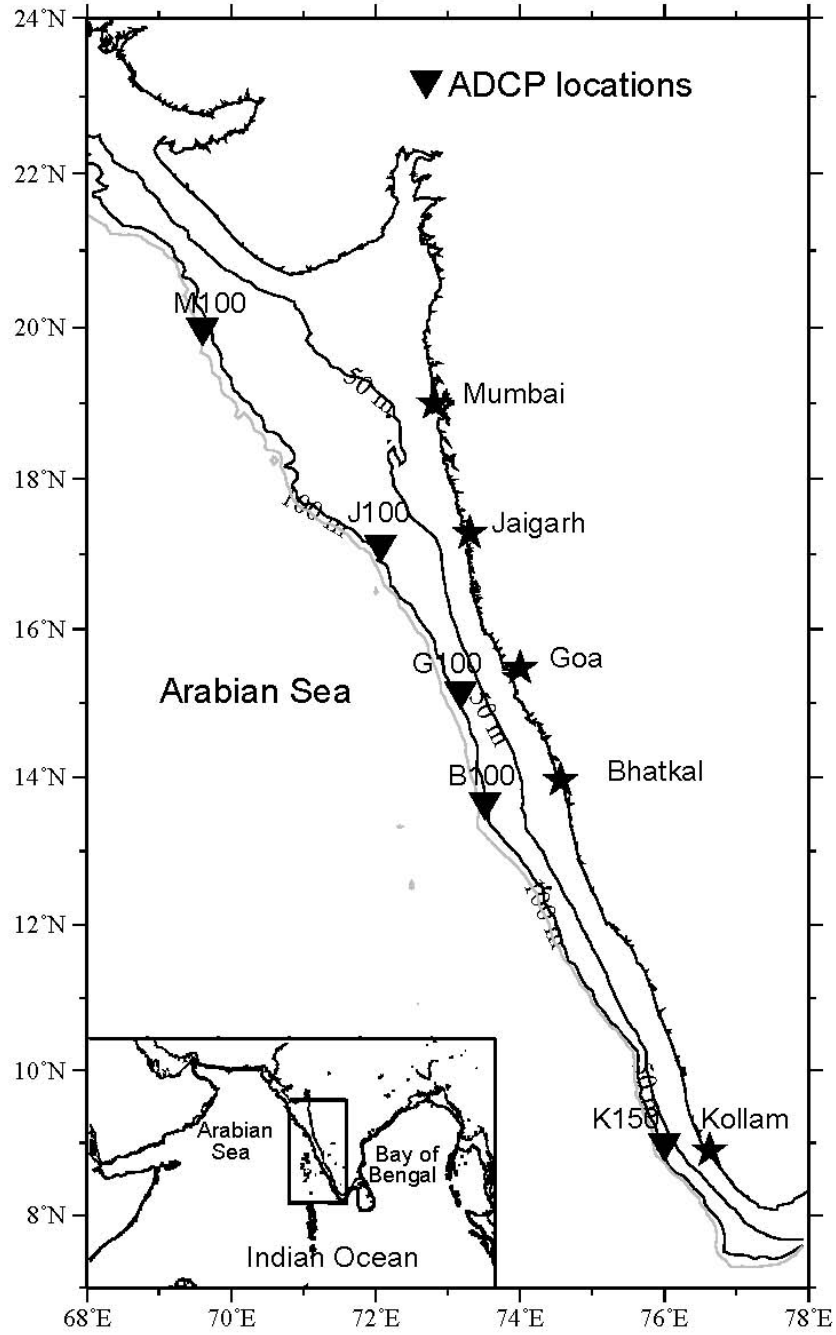


**Fig.1**

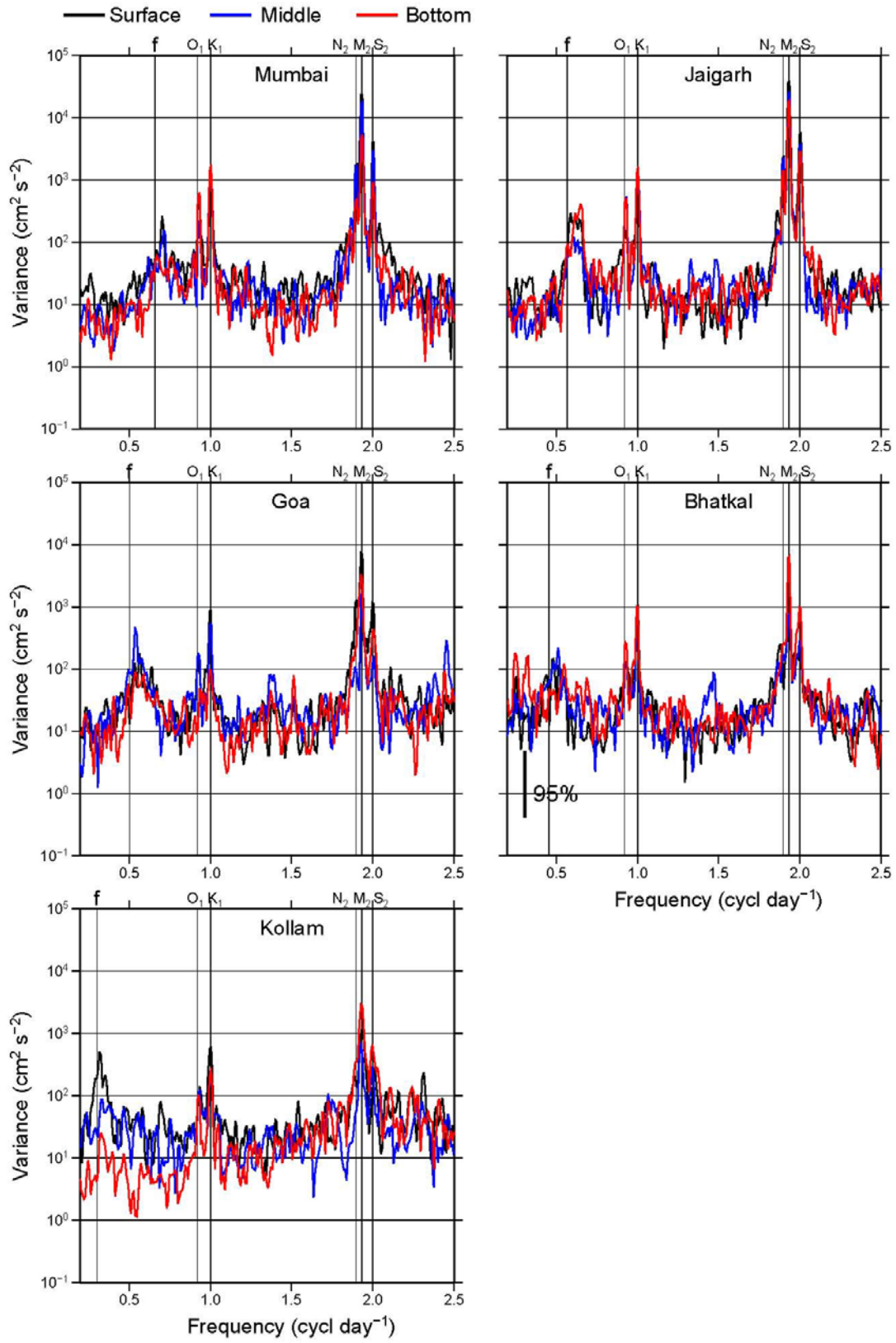


**Fig.2**

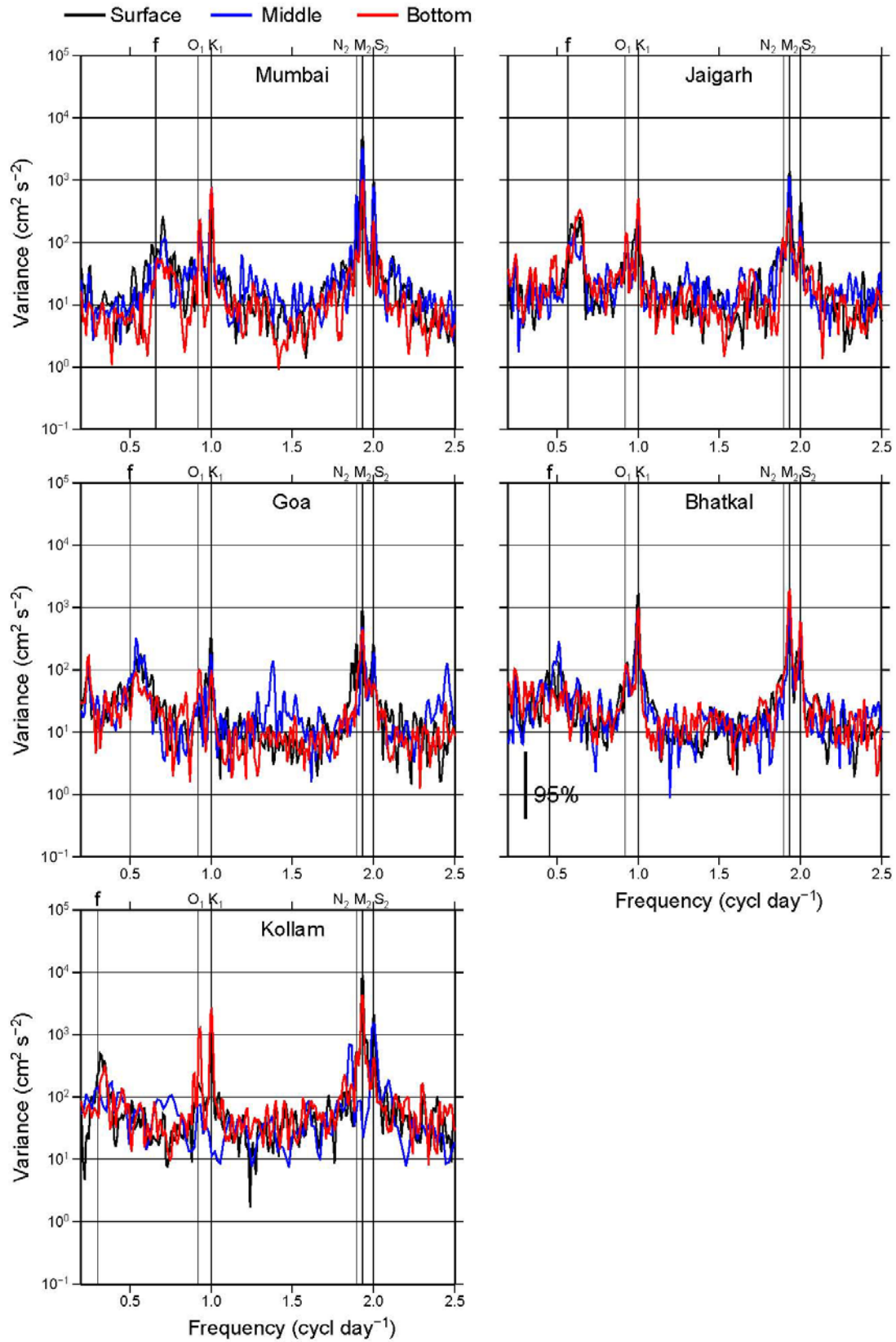


**Fig.3**

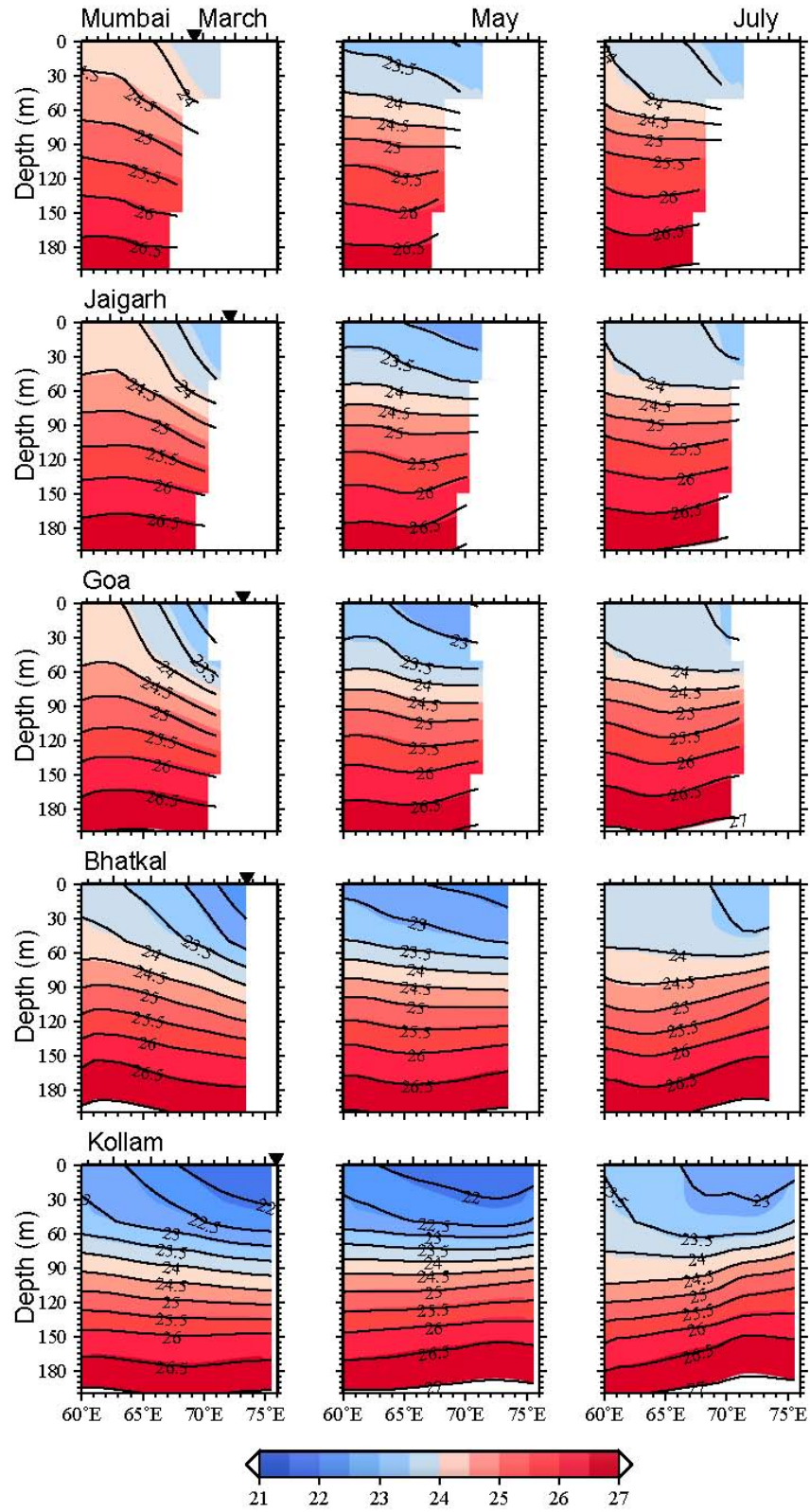
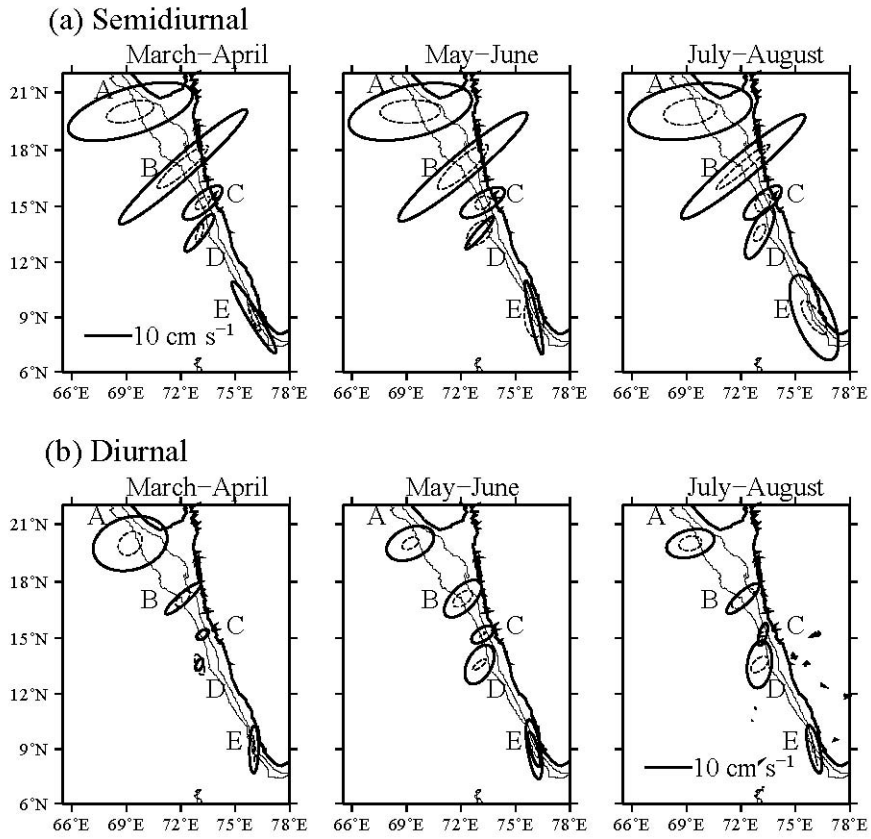
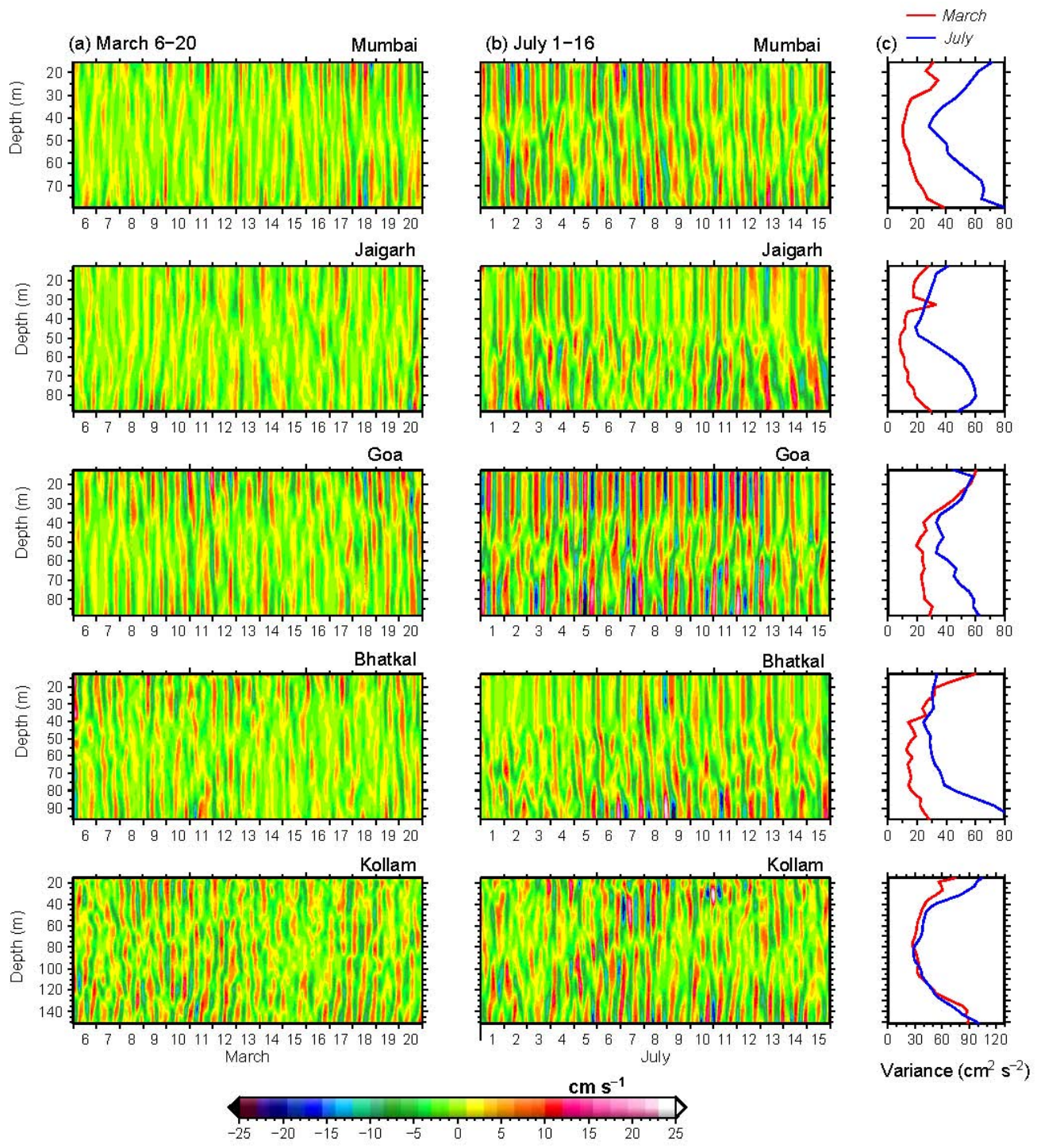


Fig.4



**Fig.5**



**Fig.6**

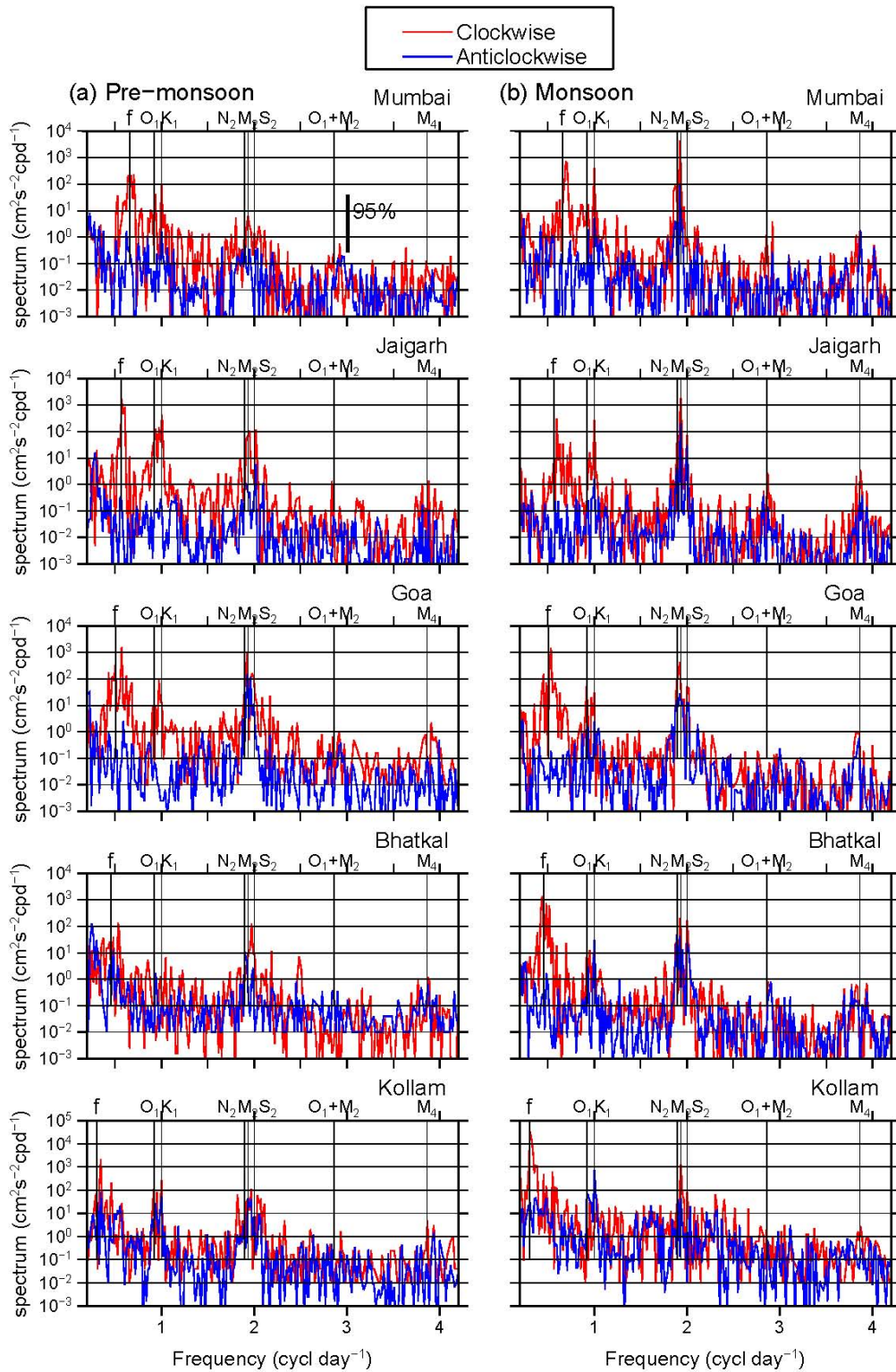


**Fig.7**



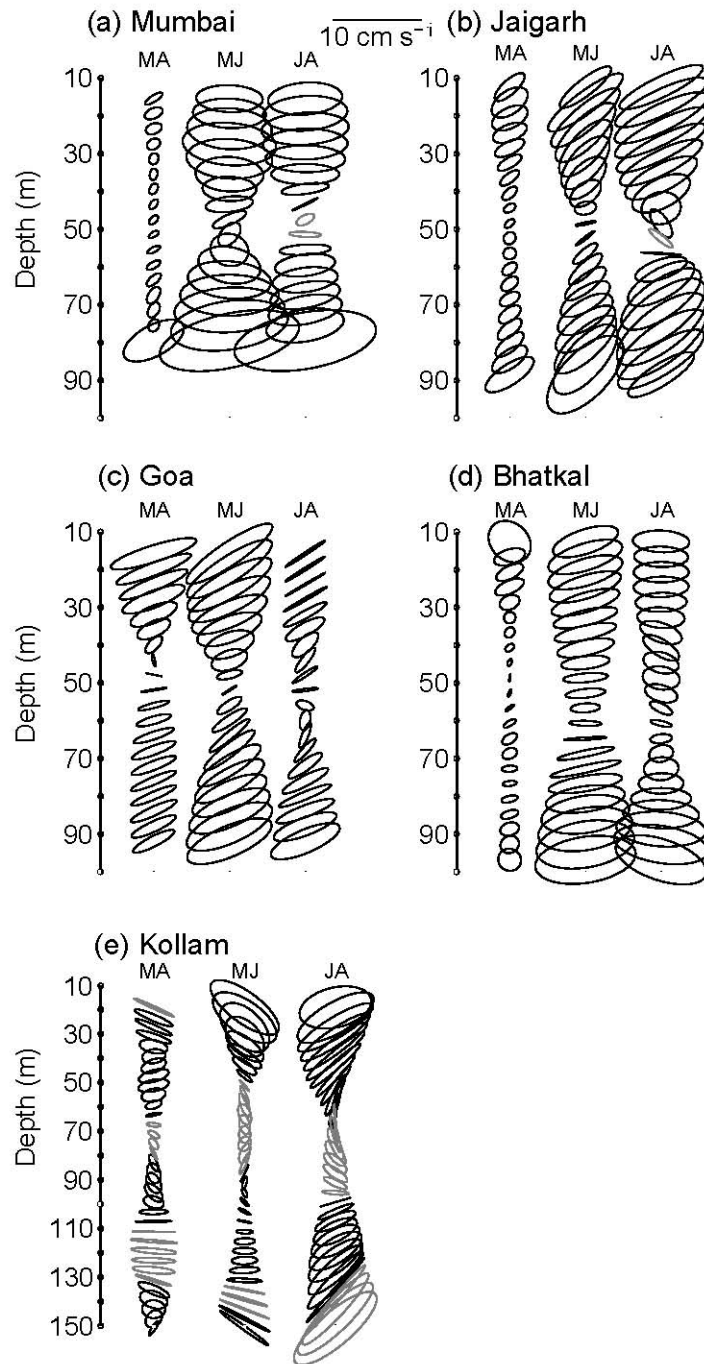


**Fig.8**

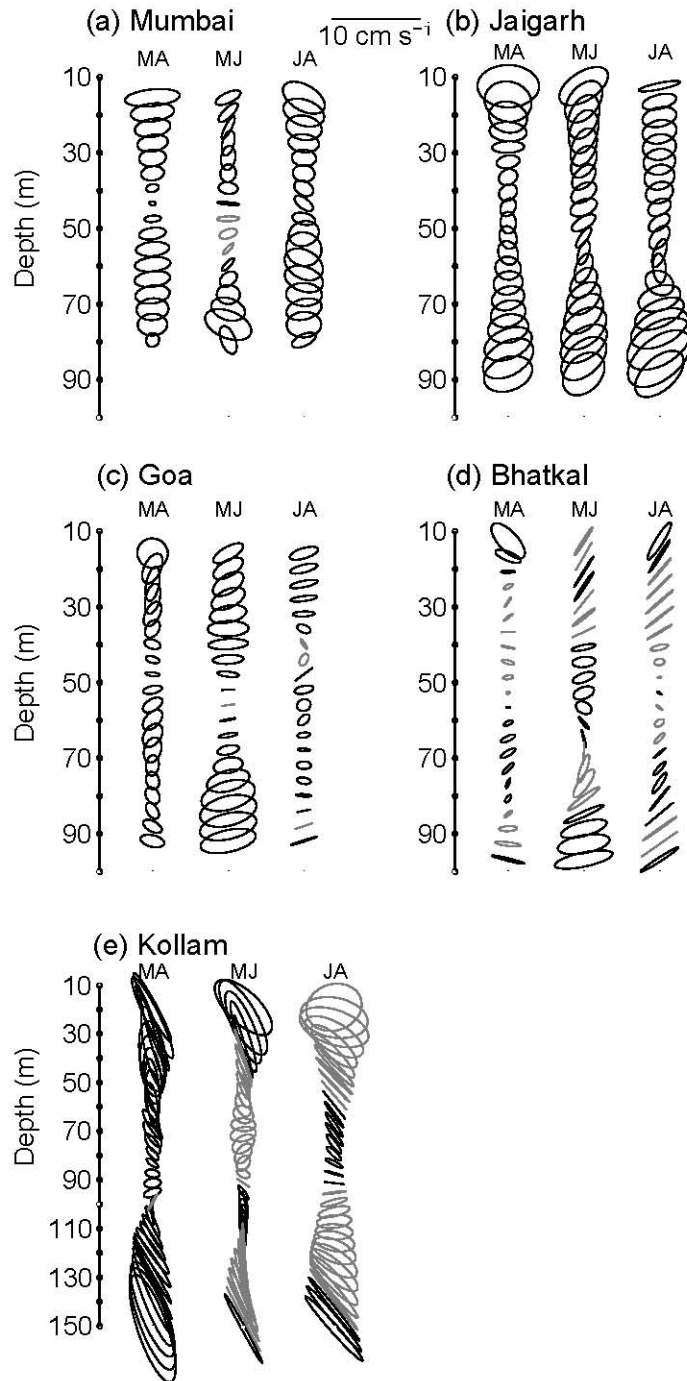


**Fig.9**

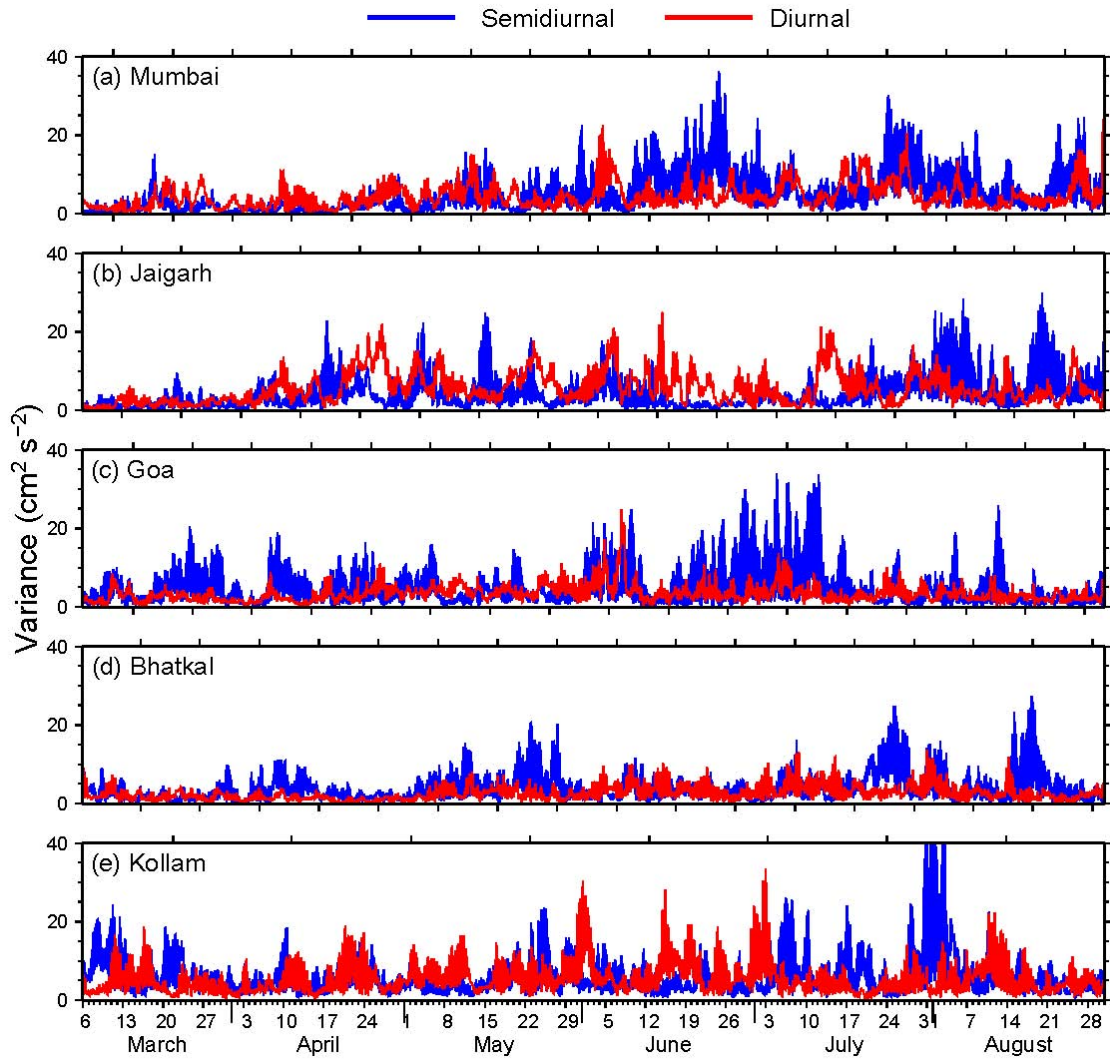


**Fig.10**

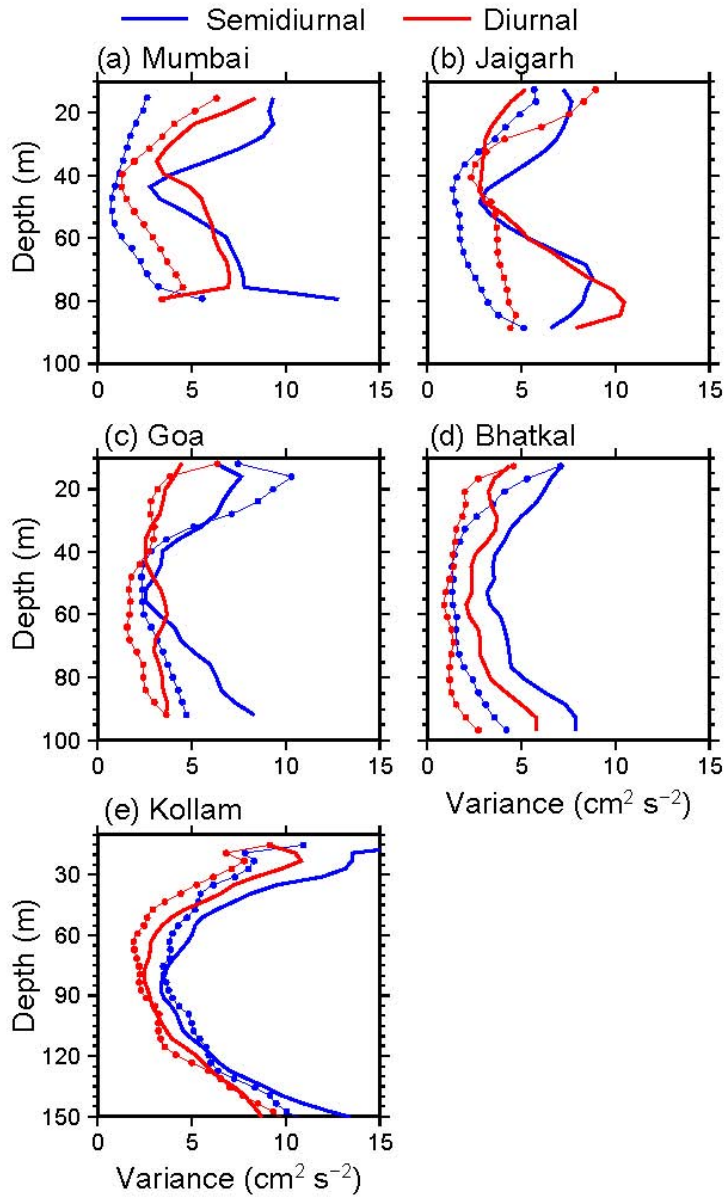


**Fig.11**

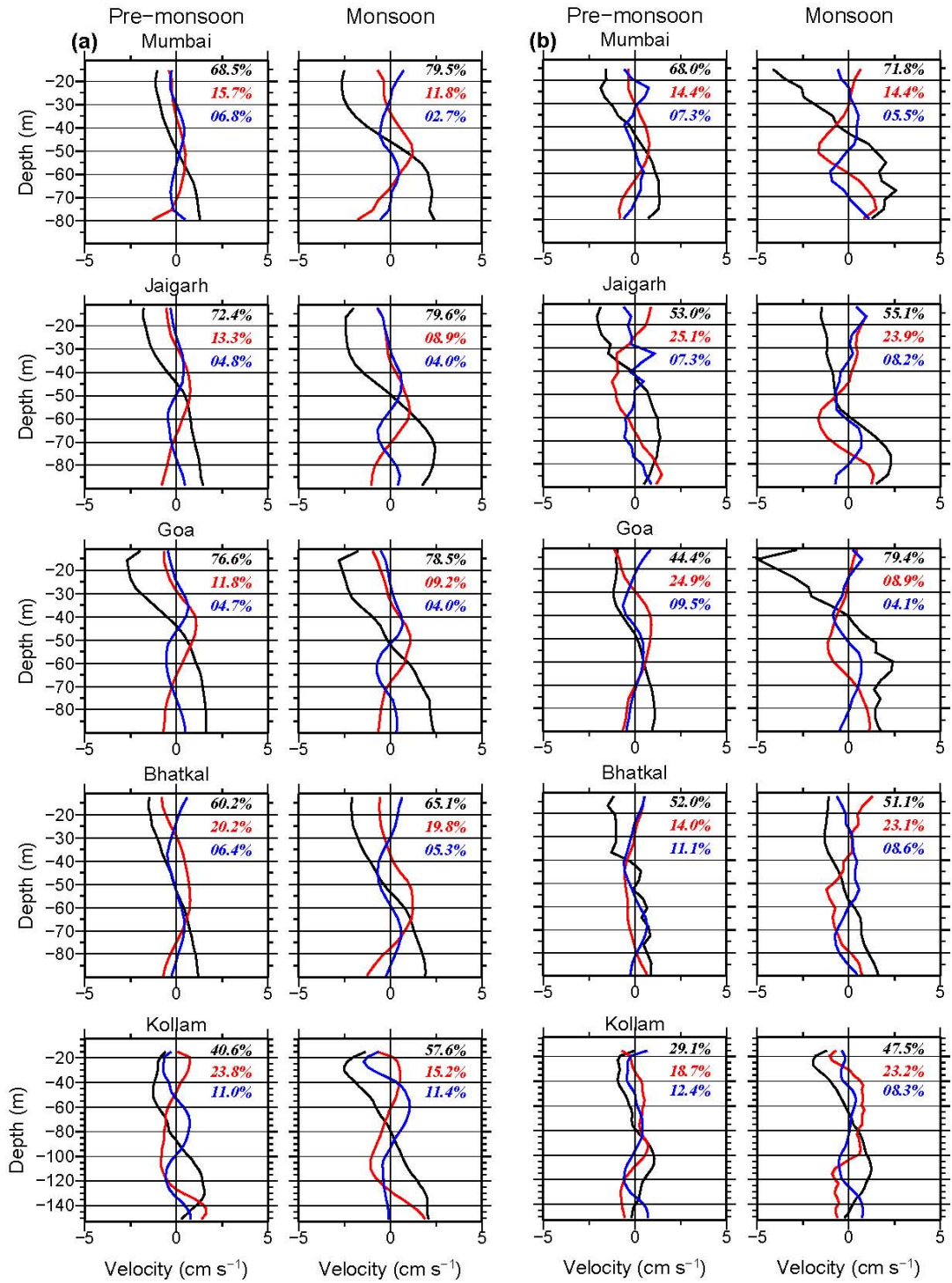
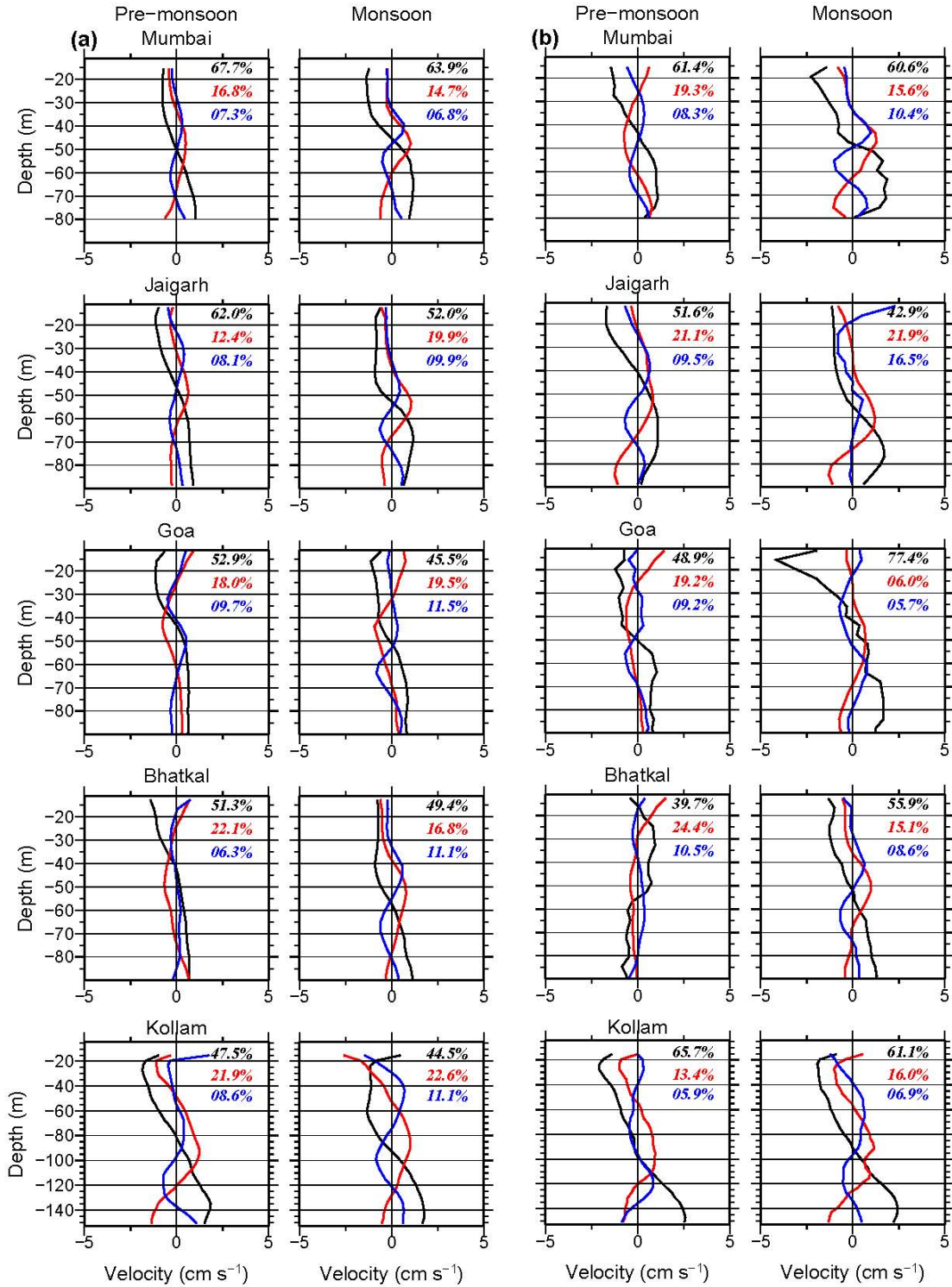
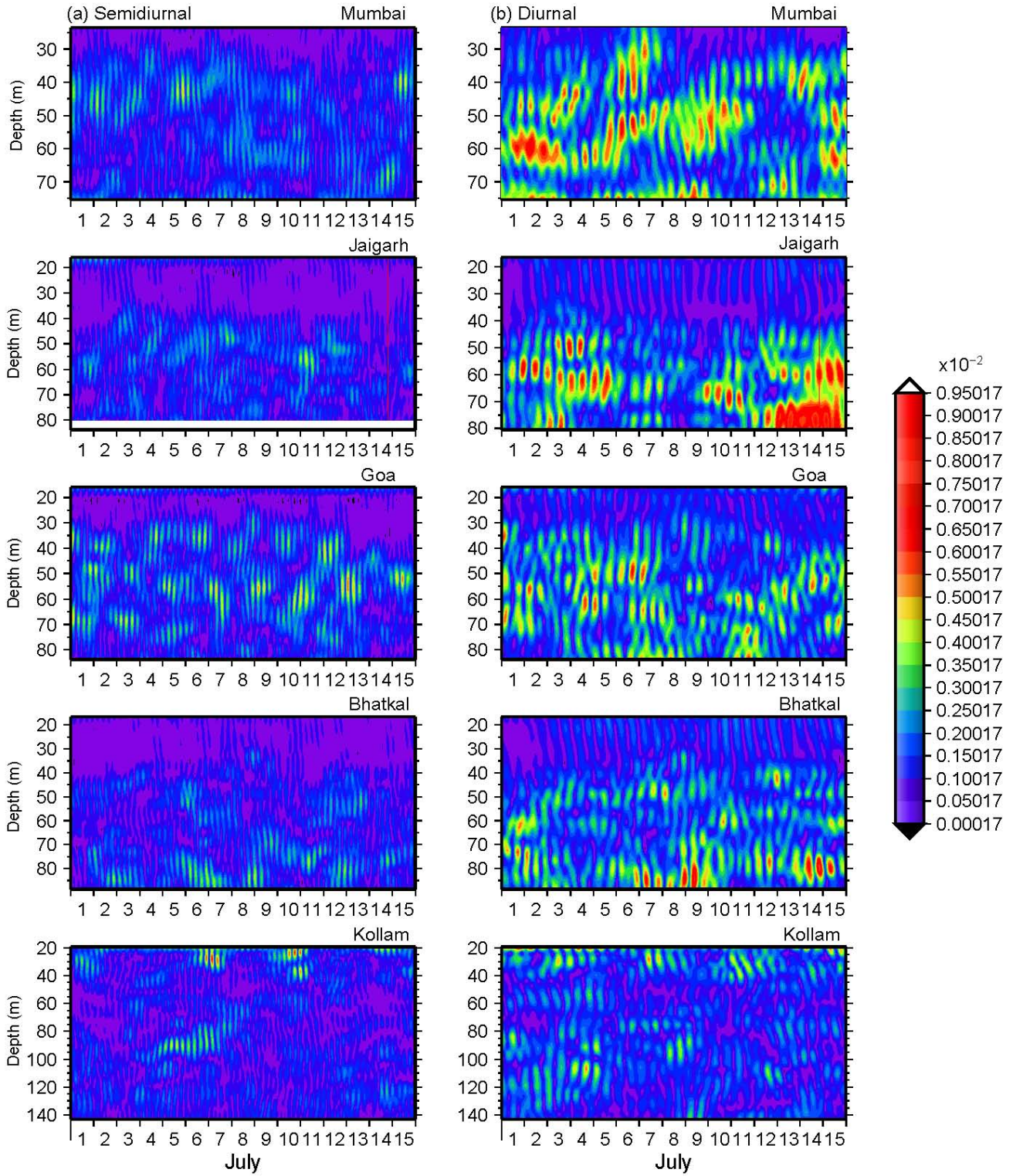


Fig.12



**Fig.13**



**Fig.14**